

**Enhancing intensity of tumor-specific fluorescence by MEK
inhibition in brain tumor models**

by Shaykat Saha

A thesis submitted to the School of Graduate Studies in partial fulfillment of
the requirements for the degree of

Master of Science in Medicine
(Cancer and Development)

BioMedical Sciences

Faculty of Medicine

February 2022

Memorial University of Newfoundland

St. John's Newfoundland and Labrador

Abstract

Fluorescence guided surgery using 5-aminolevulinic acid (5-ALA FGS), a technique widely used to resect brain tumors, relies on fluorescence signals from Protoporphyrin IX (PpIX) accumulated in cancer cells to identify and resect tumor tissue. Despite its clinical success, a major issue of 5-ALA FGS is the insufficient accumulation of PpIX in tumors, posing challenges to the surgeons to delineate tumor ends. Our previous research showed that MEK inhibition increases PpIX accumulation in cancer cells but not in normal cells. In this study, we aimed to screen different MEK inhibitors for their efficacy in promoting 5-ALA mediated PpIX accumulation in human brain cancer cell lines *in vitro*. Furthermore, we sought to develop an animal model of brain cancer to evaluate the efficacy of screened MEK inhibitors in enhancing tumor visualization *in vivo*. By conducting *in vitro* fluorescence measurements, we found that MEK inhibitors Trametinib and Selumetinib were most effective in promoting PpIX accumulation in cancer cell lines. For its consistent robust effect *in vitro*, Selumetinib was selected for evaluation in *in vivo* experiments. We successfully developed a mice brain tumor model in Balb/c mice by allografting mammary cancer 4T1 cells into the brain's right hemisphere. Preliminary 2-Photon imaging results show a substantial increase in PpIX fluorescence in mice treated with Selumetinib and 5-ALA compared to mice with vehicle (DMSO/saline) and 5-ALA treatment. These results indicate the potential use of MEK inhibitor treatment to promote PpIX fluorescence in brain tumors for improved 5-ALA FGS in clinical settings.

General Summary

Brain cancer surgeries using 5-ALA (5-ALA FGS) relies on fluorescence signal from PpIX accumulated in cancer cells to detect tumors. However, some cancer cells do not accumulate enough PpIX, making them hard to detect. Our previous research has shown that inhibition of MEK, an enzyme in the MAPK/ERK pathway, results in an enhanced accumulation of PpIX in only cancer cells. The objective of this MSc project was to screen different MEK inhibitors using brain cancer cell lines and select one that is capable of enhancing PpIX fluorescence, and evaluate if the selected MEK inhibitor can enhance tumor visualization in a mouse model of brain cancer. We found that Selumetinib was the best MEK inhibitor for enhancing PpIX fluorescence in cancer cell lines. Additionally, the preliminary results show that Selumetinib treatment substantially increased PpIX fluorescence and enhanced visualization of tumors in an animal model. Overall, the results suggest that MEK inhibitors may be used to enhance tumor detection and improve the efficacy of 5-ALA-FGS in clinical settings.

Co-authorship Statement

In this thesis, I was the primary contributor to the thesis, but acknowledgment is due to my fellow researchers. The *in vivo* brain tumor model, as described in section 2.5.2, was developed with the support of Dr. Vipin Chelakkot, a postdoctoral researcher from Dr. Kensuke Hirasawa's lab. Additionally, the 2-Photon imaging of the brain tumor samples, as described in section 2.5.4 was conducted by Dr. Matthew Parsons and his lab members. All the other experiments in the thesis were conducted by me.

Acknowledgment

I would like to thank my supervisor Dr. Kensuke Hirasawa who gave me the opportunity to do this project, and for the continuous support of my master study and related research, for his patience, motivation, and immense knowledge.

I would like to thank my committee members, Dr. Michiru Hirasawa and Dr. Matthew Parsons. Whenever I ran into a trouble spot or had a question about my research, they always guided me in the right direction. They always provided the encouragement and the advice, which incited me to widen my research from various perspectives. I would also like to thank Dr. Ann Dorward for her continuous support and guidance throughout the completion of my thesis. I would not have been able to complete my master's project without their guidance.

I thank my fellow lab mates Vipin, Maria, Kaiwen, Chantel, Joseph, Danyang, and Linyang for their support, for the days we were working together, and all the fun we have had. Special thanks to Vipin, who provided me with all the training and insight into the project. Without his input and support, this project was not possible. My friends and family back home and St John's, for their support and for making me feel better on bad days. Special thanks to Sarah Connolly for all the countless support and positive energy.

I would like to acknowledge the Canadian Institutes of Health Research for the financial support of my research.

Last but not least, I would like to express my gratitude to my family: my mother and my father. It is because of them and their never-ending support, love, encouragement, and sacrifices, all the way across the world, I am able to pursue my dream, which would not have been possible otherwise.

Table of Contents

Abstract.....	ii
General Summary.....	iii
Co-authorship Statement	iv
Acknowledgment.....	v
List of Figures.....	ix
List of Tables.....	x
List of Abbreviations and Symbols	xi
Chapter 1: Introduction	1
1.1 Cancer: A Major Health Concern	1
1.1.1 Cancer Statistics in Canada.....	1
1.1.2 Introduction to Brain Cancer	2
1.1.3 Therapeutic Options for Cancer	6
1.2 Surgery: The Gold Standard in Cancer Treatment.....	7
1.2.1 Current Challenges of Surgical Resection.....	8
1.2.2 Fluorescence Guided Surgery: A New Dawn in Cancer Treatment.....	9
1.2.3 Fluorescent Probe	10
1.2.4 Types of Fluorescent probes: Exogenous and Endogenous fluorophores	12
1.2.4.1 Endogenous Fluorescent Probe	12
1.2.4.2 Exogenous Fluorescent Probe	12
1.2.4.2.1 Non-targeted Fluorescent Probes	13
1.2.4.4.2 Targeted Fluorescent Probes.....	13
1.2.5 Selection of Fluorescent Probes for FGS	14
1.3. 5-ALA: An Exogenous Fluorophore for FGS.....	14
1.3.1 PpIX: An Intermediate of the Heme Biosynthesis Pathway	15
1.3.2 Use of 5-ALA as a PDD Agent.....	18
1.3.2.1 Accumulation of PpIX in Cancer Cells	18
1.4 Clinical Application of 5-ALA in FGS	19
1.4.1 Approval of 5-ALA FGS for Clinical Use	19
1.4.2 Administration of 5-ALA and Visualization of PpIX in Patients	20
1.5 Limitations of 5-ALA Mediated FGS	20

1.5.1 Varying Degree of PpIX Accumulation in Different Cancer Types	21
1.5.2 Heterogenous Accumulation of PpIX in Cancer Tissue.....	22
1.5.3 Ras/MEK Signalling Pathway: A Commonly Disrupted Signalling Pathway in Cancer	22
1.6. Mitogen Activated Protein Kinase (MAPK) Signaling Pathway	23
1.6.1 ERK Signaling Pathway	25
1.6.2 Role MEK Signaling Pathway in Cancer	25
1.7. Targeting MEK Pathway as a Cancer Therapy	26
1.7.1 MEK Inhibitors and Cancer Treatment	26
1.7.2 Inhibitors of MEK for Clinical Use.....	27
1.7.2.1 Trametinib	27
1.7.2.2 Selumetinib	27
1.7.2.3 Cobimetinib	28
1.7.2.4 Tak733.....	28
1.7.3 The Ras/MEK Pathway and PpIX Accumulation	30
1.8 Study Rationale	32
Chapter 2: Materials and Method.....	34
2.1 Cell Culture.....	34
2.2 Reagents	36
2.2.1 MEK Inhibitors and Their Administration Protocol.....	36
2.2.2 5-ALA and its Administration Protocol	36
2.3 Quantification of PpIX Accumulation <i>in vitro</i>	36
2.4 Western Blot	37
2.5 Animal Studies.....	40
2.5.1 Mice Strains.....	40
2.5.2 Mice Allograft Model	40
2.5.3 PpIX Fluorescence Imaging.....	41
2.6 Statistical Analysis.....	42
Chapter 3: Results	43
3.1 Screening of Different MEK Inhibitors Promoting PpIX Accumulation:.....	43
3.1.1 SNB75	43
3.1.2 SF539.....	45
3.1.3 U343	47

3.1.4 4T1.....	49
3.2 Effect of MEK Inhibition on PpIX Accumulation <i>in vivo</i>	53
3.2.1 Establishment of an Animal Model of Brain Tumor	53
3.3 Establishing Protocol for Fluorescence Microscopy	55
3.4 Tumor Imaging Using 2-Photon Microscopy	57
Chapter 4: Discussion.....	60
4.1 <i>In vitro</i> Screening of MEK Inhibitors.....	60
4.2 <i>In vivo</i> Experimental Models.....	64
4.3 Microscopic evaluation of PpIX fluorescence in brain tumors.....	65
4.5 Feasibility of MEK Inhibitors for Use in FGS Applications	68
4.6 Summary	68
Bibliography	70
Appendix.....	86

List of Figures

Figure 1: Principle of Fluorescence Emission	11
Figure 2: Overview of heme biosynthesis pathway.....	17
Figure 3: MAPK Signalling pathway.....	24
Figure 4: Schematic diagram illustrating the cellular mechanisms for increasing PpIX accumulation by MEK inhibition.....	31
Figure 5: Effect of MEK inhibitors on the PpIX accumulation in SNB75 human glioblastoma cell line induced by 5-ALA.....	44
Figure 6: Effect of MEK inhibitors on the PpIX accumulation in SF539 human glioblastoma cell line induced by 5-ALA.....	46
Figure 7: Effect of MEK inhibitors on the PpIX accumulation in U343 human glioblastoma cell line induced by 5-ALA.....	48
Figure 8: Effect of MEK inhibitors on the PpIX accumulation in 4T1 ice mammary cancer cell line induced by 5-ALA.....	51
Figure 9: MEK Inhibition resulted in reduced ERK phosphorylation in mouse mammary cancer 4T1 Cell line.....	52
Figure 10: Generation of animal model of brain tumor in Balb/c mice strain.....	54
Figure 11: Visualisation of brain tumor fluorescence <i>in vivo</i>.....	56
Figure 12: <i>In vivo</i> real time imaging of PpIX fluorescence by 2-Photon microscopy.....	58

List of Tables

Table 1: The WHO grading of central nervous system (CNS) tumors.....	5
Table 2: MEK inhibitors and their clinical applications.....	29
Table 3: Cancer cell lines.	35
Table 4: Primary and secondary antibody for western blot.....	39

List of Abbreviations and Symbols

μM	Micro molar
5-ALA	5-aminolevulinic acid
ABCB6	ATP-binding cassette super-family B member
ABCG2	ATP-binding cassette super-family G member 2
ACSF	Artificial cerebrospinal fluid
ALAD	ALA dehydratase
ALAS	ALA synthase
ATP	Adenosine triphosphate
BBB	Blood Brain Barrier
BPB	Bromophenol Blue
BW	Body Weight
CNS	Central Nervous System
CPOX	Coproporphyrinogen III oxidase
CT	Computed tomography
DNA	Deoxyribonucleic Acid
ERK	Extracellular-signal-regulated kinases
FDA	Food and Drug Administration
FECH	Ferrochelatase
FGS	Fluorescence Guided Surgery
GBM	Glioblastoma multiform
GTP	Guanosine-5'-triphosphate
HMB	Hydroxymethylbilane
HMBS	Hydroxymethylbilane synthase
HRP	Horseradish peroxidase
IP	Intraperitoneal injection
JNK	c-Jun N-terminal kinases
LPS	Lipopolysaccharides

MAPK	Mitogen-activated protein kinase
MEK	mitogen-activated protein kinase kinase
MRI	Magnetic resonance imaging
NF1	Neurofibromatosis type 1
nM	Nano molar
PBG	Porphobilinogen
PBGD	Porphobilinogen deaminase
PBGS	Porphobilinogen synthase
PDD	Photo Dynamic Detection
PDT	Photo Dynamic Therapy
PET	Positron Emission Tomography
PMSF	Phenylmethylsulfonyl fluoride
TCL	Total cell lysate
PpIX	Protoporphyrin IX
PPOX	Protoporphyrinogen III oxidase
RAF	Proto-oncogene serine/threonine-protein kinase
Ras	Reticular activating system
RIPA	Radioimmunoprecipitation assay
RSKs	Ribosomal S6 kinases
RTK	Receptor tyrosine kinase
SD	Standard deviation
SDS-PAGE	Sodium dodecyl sulfate-polyacrylamide gel electrophoresis
TBST	Tris-buffered saline with tween 20
UROD	Uroporphyrinogen III decarboxylase
UROS	Uroporphyrinogen III synthase
WHO	World Health Organization

Chapter 1: Introduction

1.1 Cancer: A Major Health Concern

Cancer is one of the major public health concerns across the globe, with tens of millions of people diagnosed with the disease every year. In 2018 cancer was the second leading cause of death globally and was responsible for about 9.6 million deaths in the same year (World Health Organization, 2018). Approximately 17 million new cancer cases were reported worldwide in 2018 and are expected to reach over 27.5 million by 2040, an increase of 61.7% from 2018 (American Cancer Society, 2018). Besides its direct impact on population health, cancer has a significant economic impact, as the annual economic cost of cancer in 2010 was estimated at approximately 1.16 trillion USD (Stewart & Wild, 2014; Yoshioka et al., 2018). Cancer will therefore continue to be a major healthcare issue in our society in the coming decades.

1.1.1 Cancer Statistics in Canada

Cancer is a leading cause of death in Canada and was responsible for over one-third of all deaths in 2016 (Canadian Cancer Statistics, 2017). In 2020, it was expected that over 225,000 new cases of cancer would be reported, and over 83,000 deaths from cancer would occur. Studies also predict that over 3,000 Canadians will be diagnosed with brain and spinal cord cancer, and over 2,500 Canadians will die in consequence (Canadian Cancer Statistics, 2019). Fortunately, the incidence of cancer-related mortality is declining in Canada. The 5-year survival rates of cancer patients have risen from 55% between 1992 to 1994 to 63% in 2012 to 2014. It is also reported that cancer prevention and control efforts have saved over 179,000 Canadian lives since 1988 (Canadian Cancer Statistics, 2017). These improvements in the survival of cancer patients are

likely due to greater cancer awareness and prevention measures and technological advances resulting in earlier diagnosis, more effective treatments, and better patient management.

1.1.2 Introduction to Brain Cancer

A tumor is an abnormal mass of tissue containing cells that grow and multiply uncontrollably. Normally the body controls the growth and division of cells through numerous genes, but tumor cells evade the mechanisms that control normal cells. Within the brain, this uncontrolled growth of cells can disrupt its normal functions. Brain tumors are divided into two main groups: Primary brain tumors and secondary brain tumors. A primary brain tumor starts in the brain and may spread to other parts of the brain or the spinal cord. Primary brain cancer accounts for about 2-3% of all new cancer cases in adults, while it is the second most common form of childhood cancer, after leukemia (American Cancer Society, 2019). Secondary brain tumors originate from cancers of other organs that metastasize to the brain through the bloodstream. In adults, secondary brain tumors are more common than primary brain tumors. Nearly 25% of patients with cancer are affected by metastatic tumors to the brain, which most commonly originates from the lung or the breast (Warnick et al., 2019; Mendez & DeAngelis, 2018).

Primary brain tumors can be further classified into benign or malignant. A benign brain tumor develops slowly, with distinct boundaries. Most benign brain tumors do not grow into nearby tissue and usually do not grow back after removal (Patel, 2020). A malignant brain tumor is cancerous with irregular boundaries, rapidly growing and spreading into nearby brain areas. It is difficult to be removed completely, accounting for their subsequent regrowth after treatment. Any tumor in the brain, whether benign, malignant, or metastatic, can all potentially be life-

threatening if located in a vital area of the brain. Due to the rigid structure of the cranium, the brain cannot expand to make room for a growing mass of tissue. As a result, the tumor can compress or displace normal brain tissue and disrupts normal brain function.

Depending on the cell type, primary brain tumors can further be classified as glioma and non-glioma tumor types. Gliomas are the most prevalent central nervous system (CNS) tumors, representing about 30% of all brain tumors and over 80% of malignant brain tumors (Goodenberger & Jenkins, 2012; Ostrom et al., 2014). They originate from the glial cells that surround and support the nerve cells. Depending on the type of glial cells, gliomas are divided into astrocytoma, oligodendroglioma, and oligoastrocytoma. Tumors that arise from astrocytes are called astrocytomas and are commonly found in the cerebrum and cerebellum. High grade astrocytomas are most prevalent in young adults and older patients, while low grade astrocytomas are common in children (Mesfin & Al-Dhahir, 2020). Tumors that arise from cells and structures of the brain that are not glial cells, such as meninges, pituitary gland, pineal gland, and cells lining the ventricles of the brain, are called non-glioma tumors. Most prevalent examples of non-gliomas include meningiomas, medulloblastomas, and primary CNS lymphomas (Marta et al., 2011; Schroeder & Gururangan, 2014).

Under the World Health Organization (WHO) grading system, brain tumors are classified into grades I to IV based on histological features of tumors as summarized in Table 1 (Altinay, 2017). These grades indicate how aggressive the tumor is likely to be (Louis et al., 2007). A higher grade is usually associated with tumors that are more aggressive and more likely to grow quickly. Glioblastoma multiforme, a grade IV astrocytoma subtype, is the most common and the most aggressive form of brain cancer, accounting for over 40% of all gliomas (Ostrom et al., 2014).

These tumors show rapid growth, spread to other tissue, and are associated with poor prognosis (Hanif et al., 2017).

Table 1: The WHO grading of central nervous system (CNS) tumors.

WHO	Features of Grading
Grade I	Have low proliferating potential and it may be possible to completely remove the tumor with surgery.
Grade II	Usually have diffuse infiltrative and low proliferating potential, but probability of low recurrence rate, some of them have risk of progression to high grade.
Grade III	Mostly known as anaplastic tumors and have malign histologic features and is likely to spread into nearby tissues. Have high recurrence rate and usually need chemotherapy and radiotherapy.
Grade IV	Obviously malign tumors, which are necrotic and have capability of fast recurrence, most of them show diffuse spreading to CNS.

Note: Adapted from “Role of Pathologist in Driver of Treatment of CNS Tumors” by S. Altinay, 2017, p. 24, In *New Approaches to the Management of Primary and Secondary CNS Tumors*. IntechOpen. [Attribution 3.0 Unported \(CC BY 3.0\)](#).

1.1.3 Therapeutic Options for Cancer

Several types of treatments are available for cancers, such as chemotherapy, radiotherapy, and surgical removal, each of which has advantages and limitations. Chemotherapy is a form of systemic therapy where drugs taken orally or injected into the body travel through the bloodstream to fight cancer cells anywhere in the body. Chemotherapy targets actively dividing cells as cancer cells proliferate and grow more rapidly than most normal cells in the body (Raguz & Yagüe, 2008). One major advantage of chemotherapy is the wide distribution of the drug throughout the body and its ability to target cancer cells that have metastasized from the primary tumor location to other parts of the body. However, as cancer-specific effects of most chemotherapy depend on the rate of cell division, the primary side effects are damaging normal cells with fast growing rates, such as those in the bone marrow, hair follicles, and digestive tract. The short-term side effects include nausea, vomiting, loss of appetite, hair loss, constipation, and diarrhea, while the long-term side effects of chemotherapy may include damage to lung tissue, heart problems, infertility, kidney problems, nerve damage, and the risk of second cancer (American Cancer Society, 2020)

A radiotherapy is a form of localized therapy using high energy beams to kill cancer cells. The high energy beam most commonly used is X-rays, but protons or other forms of high energy beams are also utilized. High-energy beams damage the genomic DNA of cells to prevent it from dividing and thus are effective against cells with high proliferation rates, such as cancer cells. As a result, radiotherapy can reduce the tumor burden or destroy it completely (National Cancer Institute, 2019). Similar to chemotherapy, radiotherapy comes with some side effects. The primary side effects of radiotherapy include fatigue, loss of appetite and skin problems and hair loss in the area being treated with radiotherapy. Additionally, late side effects of radiotherapy can appear a long time after the treatment finishes. These side effects depend on the part of the body being

radiated. They may include cavities and tooth decay, early menopause in women, cardiovascular complications, infertility, and often increase the risk of developing other types of cancer (National Health Service, 2020).

Surgical resection remains to be the cornerstone for the cure and control of most solid cancers. If all of the cancer cells can be surgically removed, the patient will be cured of that cancer (Zheng et al., 2019). Although surgery is most effective at completely removing cancer from the primary site at an early stage, it can also be used to resect secondary tumors that have metastasized to other parts of the body. While there are several reasons why a patient may undergo surgery, including cancer diagnosis, staging, prevention, and tumor debulking, the ultimate goal of surgery is to completely remove the cancerous tissue from a specific place in the body. When complete tumor removal is a challenge, debulking can effectively reduce tumor size and control its growth. Debulking can make other forms of treatment such as chemotherapy and radiotherapy more effective as it minimizes the remaining population of cancer cells that might require further treatment (Khong et al., 2014).

1.2 Surgery: The Gold Standard in Cancer Treatment

For many solid tumors, surgical resection remains the primary treatment option, as the complete removal of all cancer cells is closely tied to its curability and disease outcome (Nagaya et al., 2017). Surgical resection offers the greatest possibility of prolonged progression-free survival and an overall better patient outcome across all stages (Metildi et al., 2012). The presence or absence of tumor cells in the surrounding area of resected tissue, known as surgical margin, is a strong predictor of tumor recurrence and patient survival. A positive margin refers to the presence

of tumor cells at the cut edge of the resected tissue and is associated with high local recurrence and poor prognosis in patients. (Frankel et al., 2013; Nguyen & Tsien, 2013; O'Donnell et al., 2014).

1.2.1 Current Challenges of Surgical Resection

Although there has been a continuous effort to enhance surgical technology and techniques, complete removal of cancerous tissue is still a challenge. Despite best efforts and treatments, glioblastomas recur in almost all patients (Nguyen & Tsien, 2013). Other forms of cancer with higher recurrence rates include ovarian cancer, bladder cancer, soft tissue sarcoma, and lymphoma with 85%, 50%, 50%, and 75% recurrence rates, respectively (Primeau, 2018). To minimize the chances of tumor recurrence, a significant volume of surrounding normal tissue can be resected in some organs. However, tumor resection with a large margin is challenging in certain organs as removing or damaging any surrounding healthy tissue may interfere with normal organ functions. One such organ is the brain, where the surgeons do not have the luxury to resect surrounding normal tissues without fear of disrupting normal brain functions (Mondal et al., 2014). Therefore, it is essential to improve surgical techniques and develop new clinical tools to maximize the efficiency of tumor resection while maintaining normal organ functions for the patient's quality of life post-surgery.

To this end, several preoperative imaging techniques have been developed that generate images highlighting the structural, functional, and locational details of the cancerous tissue, including magnetic resonance imaging (MRI), computed tomography (CT), and positron emission tomography (PET) (Mondal et al., 2014). With the help of these imaging techniques, tumor detection, diagnostic accuracy, and preoperative planning have improved greatly (Wang et al.,

2015; Mabray et al., 2015). Despite these advances in imaging techniques, in providing valuable information on tumor location and characteristics, incorporating these systems into the operating room is currently a challenge due to their large hardware footprint, slow imaging speed, inability to provide microscopic details, huge cost of operation, and the need for a specialized operator (Jolesz, 2014; Vahrmeijer et al., 2013). It remains a significant challenge to develop novel surgical approaches that differentiate the normal tissue from the cancerous tissue intraoperatively. Therefore, surgeries still largely rely on visualization by the eyes of operating surgeons.

1.2.2 Fluorescence Guided Surgery: A New Dawn in Cancer Treatment

To overcome the challenges that traditional cancer surgery is facing, new medical imaging techniques have been developed to aid surgeons in identifying tumor ends during surgery. One such imaging technique is photodynamic detection (PDD), which allows surgeons to detect tumor ends by means of a fluorescence signal. The use of PDD to maximize the precision and efficacy of tumor resection is called fluorescence guided surgery (FGS) (Gioux et al., 2010; Kaneko & Kaneko, 2016; Ishizuka et al., 2011). FGS proceeds as a regular surgical process with specialized illumination of the surgical region using light of specific wavelength to excite fluorescent probe molecules that are specifically accumulated in the tumors. The emitted fluorescence is detected in real-time through a set of specialized imaging filters or lenses (Mondal et al., 2014). As FGS does not require much additional equipment in an operating room, it does not alter the surgical procedure significantly, making it a potential add-on technique to be commonly used (Allison, 2015).

1.2.3 Fluorescent Probe

Fluorescent probes are compounds that possess the intrinsic ability to emit light when excited with light of a specific wavelength. Figure 1 (Dunst & Tomancak, 2019) illustrates the mechanism of light absorption, changes in electronic configuration, and light emission from a fluorescent probe. When the fluorescent probe absorbs the light, it reaches the excited state (S_1 or S_2) from the ground state (S_0) by raising the energy level of electrons. The excited electrons remain in this high energy state for a very short period. Following this excitation state, the electrons return to the ground state (S_0) by emitting light (photons) of lower energy (longer wavelength) in the form of fluorescence. The amount of time the electrons remain in an excited state before returning to the ground state is called fluorescence lifetime and is proportional to the amount of fluorescence emission. The number of photons emitted relative to the number of photons absorbed by the fluorescent probe is the quantum yield. The process of excitation and light emission of a fluorescent probe runs in cycles until the fluorescent probe undergoes photobleaching. Photobleaching is photo-induced chemical destruction of the fluorescent probe, where the fluorescent probe permanently loses its fluorescence capacity (Vicente et al., 2007).

For FGS applications, it is essential to consider the properties of the tissue and the fluorescent probe that influence fluorescence emission from the tissue. The quantum yield of the fluorescent probe can be affected by the surrounding environment of the tumor and the depth the excitation light must travel before reaching the fluorophore. Other important predictors include the concentration and distribution of fluorescent probes in the tissue, scattering, and absorption of the fluorescence by surrounding tissue, and the nature of the tissue surface. Therefore, the fluorescent probes must be selected for FGS based on their properties that generate a strong fluorescence contrast between the tumor and adjacent tissue, which helps visualize tumor mass in real time.

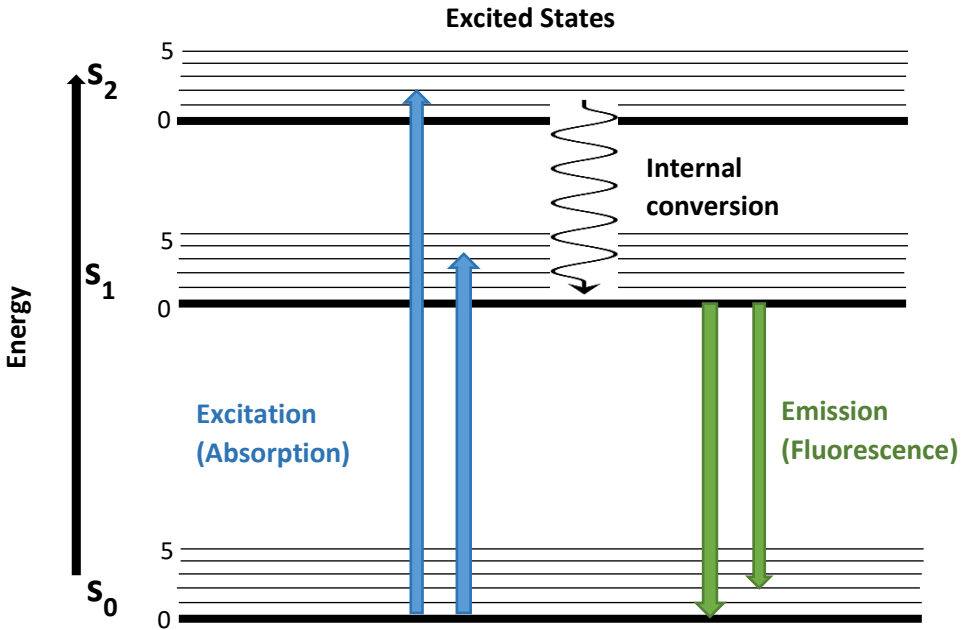


Figure 1: Principle of fluorescence emission.

Horizontal lines depict the electronic energy levels. S_0 represent the ground state. S_1 and S_2 are the first and second electronic energy levels. When the excited electrons return to their ground state, the fluorescence probe emits fluorescence. The transitions between electronic states can be nonradiative (wiggly arrows) or radiative (straight arrows).

Note: Adapted from “Imaging Flies by Fluorescence Microscopy: Principles, Technologies, and Applications,” by S. Dunst and P. Tomancak, 2019, *Genetics*, 211(1), p. 17. [Attribution 4.0 International \(CC BY 4.0\)](#).

1.2.4 Types of Fluorescent probes: Exogenous and Endogenous fluorophores

The fluorescence emitted by fluorescent probes can guide surgeons during FGS to delineate and resect tumor tissue. The fluorescent probes used in the clinical setting can be divided into two types, endogenous fluorescent probes and exogenous fluorescent probes.

1.2.4.1 Endogenous Fluorescent Probe

Endogenous fluorescent molecules are found naturally in tissues and are responsible for the fluorescent properties of biological tissues. The endogenous fluorescence of tissues upon excitation with light is called autofluorescence. These endogenous fluorophores can be classified into four groups: 1) porphyrins, 2) amino acids and proteins, 3) flavins, and 4) pyridine nucleotides. The primary benefit of using endogenous fluorescence contrast is that the patient does not need to take drugs, thus avoiding any complications such as adverse drug reactions. However, endogenous fluorophores suffer from weak quantum yield and non-specific accumulation in normal tissue, making the distinction between the tumor and normal tissue very difficult (Nguyen & Tsien, 2013).

1.2.4.2 Exogenous Fluorescent Probe

Exogenous fluorescent probes and their precursors are compounds that can be safely administered to patients. When administered, the fluorescent probe accumulates directly into the tissue or is converted from the precursor as it enters cellular pathways and accumulates into the target tissue (Borisova et al., 2014). Exogenous fluorescent probes have higher fluorescence yields compared to endogenous fluorescent probes, thereby facilitating real-time imaging and detection (Ramanujam, 2000). However, safety profiles, including drug toxicity, allergic reactions, and

photosensitivity of patients, need to be addressed. The exogenous fluorescent probes used for cancer detection can further be divided into two types, 1) Non-targeted fluorescence probes and 2) Targeted Fluorescent probes.

1.2.4.2.1 Non-targeted Fluorescent Probes

The accumulation of non-targeted fluorescent probes is not tumor-specific, but they are designed to target and accumulate in rapidly proliferating tissues (Allison, 2015). Since tumor cells proliferate at a higher rate, non-targeted fluorescence probes have found a use in FGS of tumors. The non-targeted fluorescent probes include indocyanine green, methylene blue, and fluorescein sodium which are currently used in clinical settings (Nagaya et al., 2017; Liu et al., 2021; van Manen et al., 2018)

1.2.4.4.2 Targeted Fluorescent Probes

Targeted fluorescent probes are accumulated specifically in tumors compared to in normal tissue; however, the exact mechanisms of this selective accumulation in tumors are still unknown. One of the possible explanations is poor clearance of the fluorescent probe from tumors compared to normal tissue (Huang, 2005; Matsui et al., 2010). Given their specificity for tumors, many targeted fluorescent probes have been used in FGS, including photofrin, foscan, verteporfin and texaphyrin (Baskaran et al., 2018).

1.2.5 Selection of Fluorescent Probes for FGS

The success of FGS depends on the type of fluorescent probe used to visualize tumors. To achieve a tumor-specific fluorescence during FGS, several properties of the fluorescent probe need consideration. First, the fluorescent probe should accumulate selectively in tumors and not normal tissue. Second, the fluorescent probe must not be harmful to normal tissues and have a short half-life, so that it clears from tissues within hours or days to prevent toxic effects but allow enough time for tumor visualization. Third, it should be easy to integrate into the surgical procedure without introducing too much additional complexity. Lastly, the fluorescent probe should have a high quantum yield, leading to a distinct difference in fluorescence emissions between tumor and normal tissue, allowing surgeons to differentiate tumor from normal tissue (Allison, 2015; Sevick-Muraca & Rasmussen, 2008).

1.3. 5-ALA: An Exogenous Fluorophore for FGS

Among existing fluorescent probes, 5-aminolevulinic acid (5-ALA) is the most widely used in clinical settings. During 5-ALA FGS, exogenous 5-ALA administered into the patient results in an elevated production and accumulation of PpIX in cells. PpIX is an endogenous fluorescent agent that is accumulated more efficiently in cancer cells than normal cells, making 5-ALA an excellently targeted probe for FGS of tumors (Nagaya et al., 2017). 5-ALA is clinically used for the PDD of the brain, bladder, and gastric cancers (Hadjipanayis & Stummer, 2019; Millon et al., 2010; Inoue, 2017). In addition, 5-ALA is used in photodynamic therapy (PDT) to eliminate cancer cells. During PDT, PpIX acts as a photosensitizer and produces oxygen species that kill tumor cells when exposed to the light of specific wavelengths, such as red visible light

(600-740 nm) and green visible light (450-580 nm) (Collaud et al., 2004; Inoue, 2017).

1.3.1 PpIX: An Intermediate of the Heme Biosynthesis Pathway

While 5-ALA can be administered exogenously for FGS and PDT to treat cancer, it is also found endogenously as a key molecule for heme biosynthesis. The heme biosynthesis pathway is a multi-step process involving different intracellular compartments, starting with the production of 5-ALA and ending with the conversion of PpIX into heme (Figure 2) (Wachowska et al., 2011). The first step in the heme biosynthesis pathway is the synthesis of 5-ALA from glycine and succinyl CoA by ALA synthase (ALAS) on the inner mitochondrial membrane (Ponka, 1999; Yang et al., 2015). The second step involves the transfer of 5-ALA to the cytosol, where porphobilinogen (PBG) is formed by condensing two molecules of 5-ALA, catalyzed by an enzyme called ALA dehydratase (ALAD). Next, hydroxymethylbilane (HMB) is generated by condensing four molecules of PBG, the first tetrapyrrole in the pathway, which is catalyzed by the enzyme porphobilinogen deaminase (PBGD). PBGs lose their amino acids when they form a linear tetrapyrrole HMB. The linear tetrapyrrole HMB is then catalyzed by the enzyme uroporphyrinogen III synthase (UROS) to form cyclic uroporphyrinogen III, decarboxylated by Uroporphyrinogen III decarboxylase (UROD), leading to the formation of coproporphyrinogen III. Coproporphyrinogen III is then transferred back into mitochondria, where it undergoes oxidative decarboxylation by coproporphyrinogen III oxidase (CPOX) to generate protoporphyrinogen III. Furthermore, protoporphyrinogen III is oxidized by protoporphyrinogen III oxidase (PPOX) to produce PpIX. The final step in the heme biosynthesis pathway is the chelation of PpIX by an iron (II) to form heme in mitochondria, catalyzed by the enzyme ferrochelatase (FECH) (Wachowska et al., 2011). PpIX possesses fluorescence and photosensitizing activity that can be used for PDD

and PDT, while heme does not (Stummer et al., 2000). PpIX is also effluxed out from the cells through the members of the ATP binding cassette family of transporters, including ATP-binding cassette super-family G member 2 (ABCG2) and ATP-binding cassette super-family B member 1 (ABCB1) (Yoshioka et al., 2018; Yang et al., 2015).

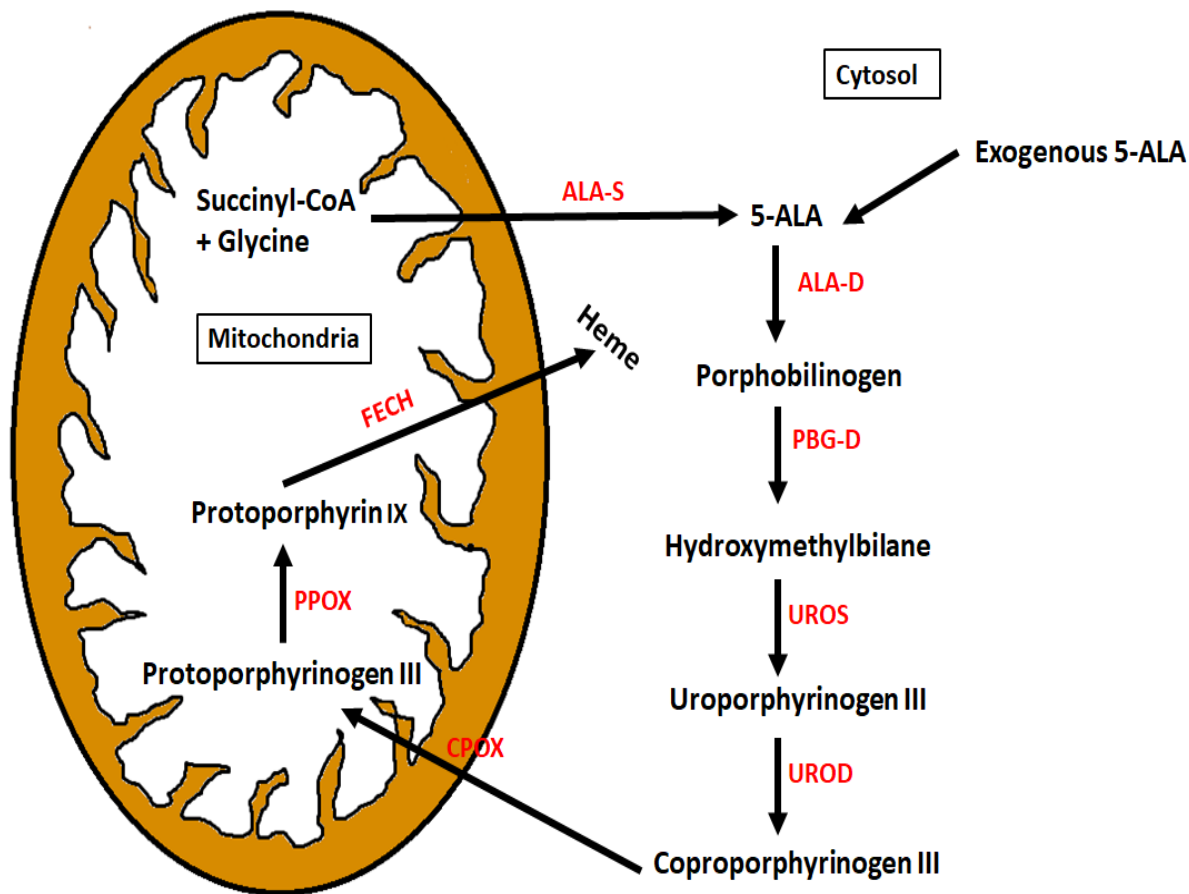


Figure 2: Overview of the heme biosynthesis pathway.

5-ALA is a non-fluorescing photosensitizer precursor and an intermediate in the heme biosynthesis pathway. The rate-limiting step of this pathway is the synthesis of endogenous 5-ALA by the enzyme ALAS. Thus, the exogenous administration of 5-ALA bypasses this rate-limiting step. 5-ALA is converted to strongly fluorescing protoporphyrin IX through a series of enzymatic processes prior to the final step of conversion to heme within mitochondria.

ALA-S: 5-aminolevulinic acid synthase, FECH: Ferrochelatase ALA-D: 5-aminolevulinic acid dehydratase, CPOX: Coproporphyrinogen oxidase, PBG-D: Porphobilinogen deaminase, PPOX: Protoporphyrinogen oxidase, UROD: Uroporphyrinogen decarboxylase, UROS: Uroporphyrinogen III synthase.

Note: Adapted from “Aminolevulinic acid (ala) as a prodrug in photodynamic therapy of cancer,” by Wachowska, M., Muchowicz, A., Firczuk, M., Gabrysiak, M., Winiarska, M., Wańczyk, M., Bojarczuk, K. and Golab, J., 2011, *Molecules*, 16(5), p. 41440. [Attribution 3.0 Unported \(CC BY 3.0\)](#).

1.3.2 Use of 5-ALA as a PDD Agent

The first use of exogenous 5-ALA for the detection of gliomas was first reported in 1998 (Stummer et al., 1998). The finding led to the establishment and development of concepts of PpIX application to FGS. The ability of a 5-ALA metabolite PpIX to distinguish normal tissue from the tumor in different types of organs has made it a great candidate for PDD (Millon et al., 2010). Additionally, 5-ALA is a safe drug, with only short-term photosensitivity of the skin and eyes reported in patients after system application of 5-ALA (Tonn & Stummer, 2008; Georges et al., 2019). This low risk of side effects associated with 5-ALA was another reason for its success in clinical settings.

1.3.2.1 Accumulation of PpIX in Cancer Cells

The cellular level of PpIX induced by exogenous 5-ALA is dependent upon a balance of factors that either increase PpIX accumulation or reduce it. The increase in PpIX accumulation is mediated through the uptake of 5-ALA into the cell and rate of synthesis of PpIX, while PpIX level is reduced through the conversion to heme and efflux from membrane transporters (Kobuchi et al., 2012). Although the mechanism underlying the selective accumulation of PpIX in cancer cells is still not fully understood, it is believed that oncogenic transformation changes the activity of enzymes in the heme biosynthesis pathway, which contributes to the enhanced PpIX accumulation in cancer cells (Yang et al., 2015). Studies have reported a decreased activity of FECH in malignant cells, resulting in a reduction in the conversion of PpIX to heme and an increase in the accumulation of PpIX (Adjei et al., 2017; Pichlmeier et al., 2008; Zhou et al., 2005). Furthermore, due to the increased metabolic rate, tumor cells suffer from a decreased cellular supply of iron, limiting the insertion of irons to PpIX that is essential for the conversion to heme

(Ishizuka et al., 2011). Oncogenic transformation has also been reported to enhance the activity of other enzymes in the heme biosynthesis pathway, such as ALAD, UROD, and PBGD (Wachowska et al., 2011; Yang et al., 2015). Other factors involved in the enhanced PpIX accumulation in cancer cells are disruptions of mitochondrial functions and alterations in the activity of porphyrin transporters such as ABCG2 and ATP-binding cassette super-family B member 6 (ABCB6) (Yang et al., 2015).

1.4 Clinical Application of 5-ALA in FGS

1.4.1 Approval of 5-ALA FGS for Clinical Use

Due to extensive research and success in clinical studies, 5-ALA FGS is now widely used for the visualization and treatment of different types of cancer in clinics all around the world (Goryaynov et al., 2019; Ishizuka et al., 2011; Roberts et al., 2012; Stummer et al., 2006; Wang et al., 2013). The European Union granted clinical approval of 5-ALA for PDD of cancers of the brain, bladder, and skin. (Millon et al., 2010). In 2017, the FDA approved 5-ALA as an intraoperative visualizing agent for FGS of high grade gliomas in the USA (Hadjipanayis & Stummer, 2019). 5-ALA FGS has shown its effectiveness in the treatment of high grade gliomas. Tsugu et al. (2011) found that 5-ALA FGS resulted in complete resection of gliomas (presence of no residual contrast-enhancing tumor on early postoperative MRI) in about 60% of all cases compared to in only 30% of standard surgery under white light. In addition, the higher frequency of complete tumor resection with 5-ALA FGS also translates to a higher 6-month progression free survival rate in patients (Stummer et al., 2006). At 6 months, the progression free survival was 21% for patients operated under white light and 41% for patients treated with 5-ALA. Moreover,

5-ALA FGS has been approved to remove intracranial brain tumors in Europe, Australia, Canada, Japan, and the USA (Polikarpov et al., 2020). Overall, 5-ALA FGS can be easily incorporated into traditional surgery techniques with limited side effects and could result in higher rates of complete tumor resection. Therefore, 5-ALA FGS will be an essential and standard surgical technique for patients with malignant gliomas in the near future (Guyotat et al., 2016).

1.4.2 Administration of 5-ALA and Visualization of PpIX in Patients

The patients are orally administrated with 20 mg/kg body weight (BW) of 5-ALA to promote PpIX accumulation in tumors a few hours before the surgery (Pichlmeier et al., 2008). During the surgery, a blue light (405nm excitation) is used to visualize the tumors emitting a red PpIX fluorescence at 635 nm (Stummer et al., 1998). 5-ALA is a safe drug, but possible side effects include short-term sensitivity of the skin and eyes (Tonn & Stummer, 2008). Therefore, it is advised that patients are not exposed to sunlight or strong artificial light within 24 hours of drug intake to prevent skin irritation or eye damage.

1.5 Limitations of 5-ALA Mediated FGS

As seen in other cancer therapeutics, 5-ALA FGS has its limitations, which remain to be solved. PpIX accumulation varies among different cancer types and different tumor grades (Silva et al., 2015). The location of the tumors can be another limiting factor as the FGS light cannot excite PpIX fluorescence if the tumors are located inside organs. Furthermore, the fluorescence signal in tumors can be photobleached with excessive light exposure, limiting the duration which allows surgeons to visualize tumors effectively.

Another limitation of 5-ALA-PDD is the occurrence of false positives, which is defined as the presence of fluorescence in normal tissues (Kaneko & Kaneko, 2016). False positive results affect the specificity of 5-ALA-PDD. Conversely, some tumors are not very sensitive to 5-ALA-PDD and show a low PpIX fluorescence or an absence of fluorescence despite the histological confirmation of malignant tissues. (Moiyadi et al., 2014). A study by Kaneko & Kaneko (2016) reported the specificity of 5-ALA mediated resection of malignant gliomas to be about 92% and the sensitivity of 86%. Their study found the presence of fluorescence in 3 samples out of the 39 non glioma tissue samples tested and the absence of fluorescence in 25 samples out of the 178 glioma tissue samples tested. Finally, as mentioned above, 5-ALA administration causes short-term photosensitivity in the skin, and the eyes may become sensitive to light (Tonn & Stummer, 2008). These are the current limitations of 5-ALA use to detect tumors in patients, which need to be addressed to improve the efficacy of 5-ALA-PDD.

1.5.1 Varying Degree of PpIX Accumulation in Different Cancer Types

One of the limitations of 5-ALA-PDD is related to the grade of cancer. High grade gliomas (WHO IV) show a heightened sensitivity to 5-ALA induced PpIX fluorescence, while low grade gliomas (WHO I and II) show very low levels of PpIX accumulation and are often not visible (Hendricks et al., 2018). Several studies have reported that tumor visualization was achieved only in 10-20% of lesions due to the low levels of PpIX accumulation in low grade gliomas (Hendricks et al., 2018; Jaber et al., 2016). Another study demonstrated that PpIX fluorescence was accumulated over 10 times more in grade IV glioblastoma than in grade II (Kaneko & Kaneko, 2016). Thus, the low accumulation of PpIX in low grade glioma limits its use as a fluorescent probe to resect low grade gliomas (Zhao et al., 2013; Valdés et al., 2011).

1.5.2 Heterogenous Accumulation of PpIX in Cancer Tissue

Another limitation of 5-ALA FGS is a heterogenous accumulation of PpIX within tumor tissue. PpIX accumulation is influenced by the location of tumor cells and the density and size of the tumor mass. Moreover, due to the intra-tumor heterogeneity, characterized by the presence of subpopulations of cells with distinct genomic alterations and components of the tumor microenvironment, PpIX fluorescence within the tumor may not be ubiquitous (Becker et al., 2021). Stummer et al. (2000) noted the presence of two types of fluorescent tissue within a tumor: a solid tumor with a vivid fluorescence and infiltrating tumor projections into normal tissue with less fluorescence. Additionally, small satellite tumors around the primary tumor have limited PpIX accumulation. Therefore, the PpIX fluorescence signal is often not strong enough, resulting in visualization difficulties (Guyotat et al., 2016). The heterogenous accumulation of PpIX may result in incomplete resections of gliomas leading to increased rates of tumor recurrence (Metildi et al., 2012).

1.5.3 Ras/MEK Signalling Pathway: A Commonly Disrupted Signalling Pathway in Cancer

To overcome the limitations of 5-ALA FGS, a better understanding of the cellular mechanisms contributing to PpIX accumulation in cancer cells is warranted. Since PpIX accumulation is commonly elevated in skin, bladder, gastric, lung, colon, and brain cancer, it is crucial to investigate the association of elevated PpIX accumulation with other commonly disrupted signaling pathways in cancer cells (Kitajima et al., 2019).

A mutation that is commonly found in human cancer cells is activating mutations in the Ras signaling molecule, found in approximately 30% of all human cancers (Schubbert et al., 2007).

Ras is a pro-oncogene, which transduces extracellular signals to the nucleus and regulates cell proliferation, differentiation, and survival (Rocks et al., 2006). Additionally, activating mutations are also found in the downstream elements of Ras in a majority of cancer cells (Santarpia et al., 2012). One such downstream element of the Ras signaling pathway is mitogen-activated protein kinase kinase (MEK) which has been shown to regulate the heme biosynthesis pathway (Yoshioka et al., 2018).

1.6. Mitogen Activated Protein Kinase (MAPK) Signaling Pathway

MAPK is a family of kinases that play a crucial role in the transduction of extracellular signals involved in important cellular processes such as regulation of gene expression, proliferation, differentiation, stress responses, apoptosis, and immune defense (Grimaldi et al., 2017). The MAPK signaling pathway is activated through a number of initiating signals, including growth factors, hormones, and cytokines, and through the Ras and Rho families of small GTPases (Roberts & Der, 2007). Figure 3 shows the three main families of the MAP kinases (Lee, Rauch & Kolch, 2020). In mammals, these are Extracellular-signal-regulated kinases (ERK), the c-JUN N-terminal kinase 1, 2 and 3 (JNK1/2/3), and p38 MAPK family of isoforms (α , β , δ , and γ) (Soares-Silva et al., 2016).

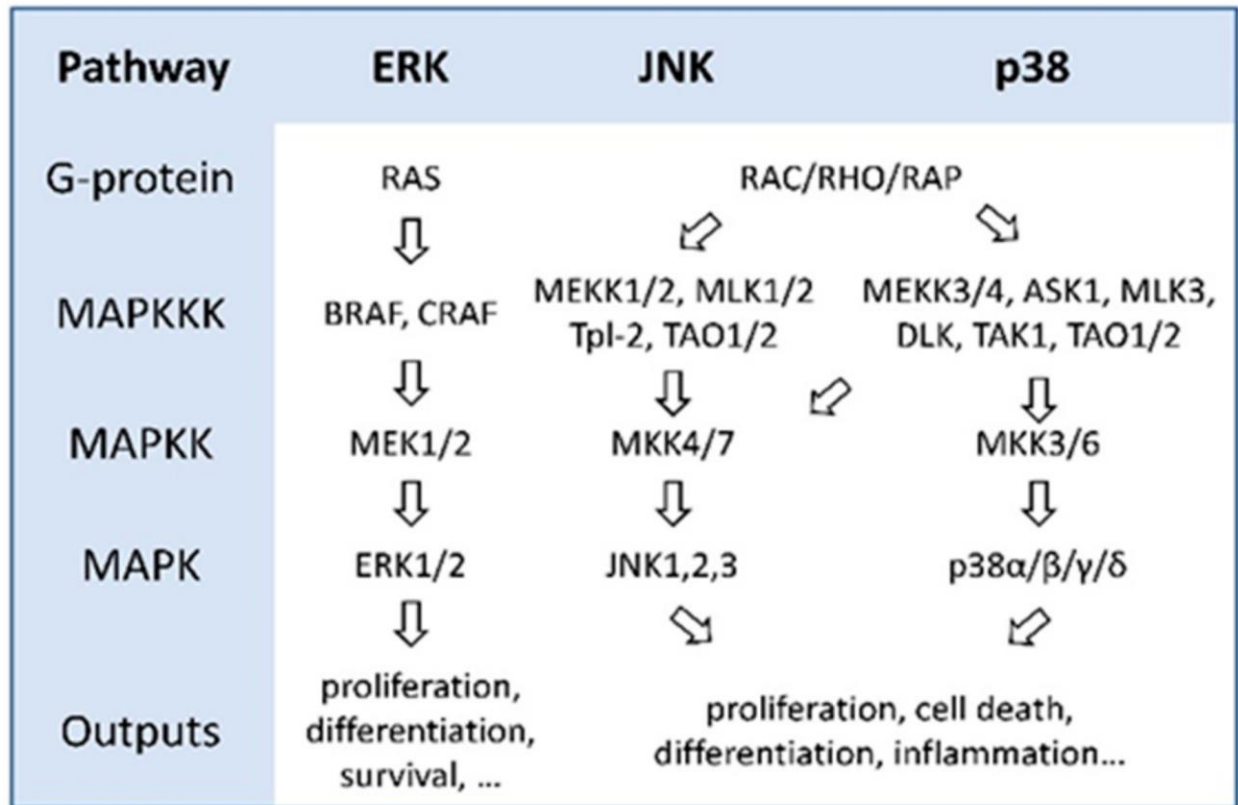


Figure 3: MAPK signalling pathway

The three well-characterized mammalian MAPK families consist of ERK, p38, and JNK signaling pathways. The MAPK signaling pathways are activated by extracellular or intracellular stimuli, upon which they activate other intracellular signaling pathways. When activated, MAPKs activate a variety of substrate proteins, including transcription factors. These transcription factors, in turn, regulate a host of cellular activities, including cell proliferation, differentiation, migration, and cell death.

Note: Reprinted from “Targeting MAPK signaling in cancer: mechanisms of drug resistance and sensitivity” by S. Lee, J. Rauch and W. Kolch, 2020, *International Journal of Molecular Sciences*, 21(3), 1102. [Attribution 4.0 International \(CC BY 4.0\)](https://creativecommons.org/licenses/by/4.0/).

1.6.1 ERK Signaling Pathway

One of the best characterized Ras downstream pathways is the Ras/MEK pathway (Zhao & Adjei, 2014). Activated Ras-GTP binds to downstream effector targets, one of which is Raf (Shaul & Seger, 2007). Raf further induces serine and threonine phosphorylation of MEK 1 and 2, which in turn activate the ERK kinase family (ERK 1 and 2). The pathway is activated in response to growth factors, pro-inflammatory stimuli, and mitogens. Activated ERK1/2 regulates several transcription and translation factors, nuclear and cytoplasmic effector genes involved in cell proliferation, differentiation, motility, angiogenesis, and cell death (Chambard et al., 2007; Knight & Irving, 2014).

1.6.2 Role MEK Signaling Pathway in Cancer

The abnormal activation of the MEK pathway has been found in many malignant tumors (Liu et al., 2018). In addition to the active mutation of Ras mentioned above, BRAF, an isoform of RAF protein kinase, has been identified as a proto-oncogene, which mutations are found in about 7% of all human cancers (Liu et al., 2018). MEK pathway plays a critical role in malignant transformation and contributes to tumorigenesis (Dhillon et al., 2007). As the MEK pathway is activated in high percentages of cancer cells and deeply involved in cancer progression, it has been studied as a therapeutic target of cancer in the field of molecular biology, biochemistry, structural biology, and cell biology (Luke et al., 2014).

1.7. Targeting MEK Pathway as a Cancer Therapy

1.7.1 MEK Inhibitors and Cancer Treatment

MEK is a kinase molecule that possesses a unique pocket structure adjacent to the ATP-binding site, which is the inhibitory binding site (Fischmann et al., 2009; Liang et al., 2011). Binding an inhibitor to the pocket induces a series of conformational changes of MEK, which prevents MEK1/2 from phosphorylation (Ohren et al., 2004). Since this mechanism does not inhibit the highly conserved ATP-binding pocket commonly present in other protein kinases, it is specific and avoids the undesired side effects (Zhao & Adjei, 2014). Several studies demonstrated the efficacy of MEK inhibitor treatment in cell cycle arrest, inhibiting tumor growth, inducing apoptosis, and reducing tumorigenicity in various tumors (Duncia et al., 1998; Hawkins et al., 2008; Zhou et al., 2014). In addition, MEK inhibitors can be used to sensitize cancer cells to other drugs and overcome drug resistance commonly seen in cancer patients undergoing chemotherapy (Vanneman & Dranoff, 2012). Table 2 lists the MEK inhibitors used in our study and their applications.

The first generation of the MEK inhibitors were PD98059 and U0126, which are highly specific to MEK1 and 2 (Santarpia et al., 2012). *In vitro* and *in vivo* studies of PD98059 indicated that its anticancer effects are due to inhibition of cell proliferation and promotion of apoptosis in solid tumors (Moon et al., 2007). U0126 is a potent and selective non-ATP-competitive MEK inhibitor. It was one of the first MEK inhibitors developed with very low off-target effects (Neuzillet et al., 2014). U0126 treatment promotes cell cycle arrest, inhibits cancer cell lines' growth *in vitro*, and reduces tumor growth in animal models *in vivo* (Yip-Schneider et al., 2003; Gysin et al., 2005; Marampon et al., 2009). U0126 is now widely used in academic research to better understand the role of RAS/MEK pathway in various malignancies (Neuzillet et al., 2014;

Cheng & Tian, 2017). However, despite their specificity, the poor pharmacodynamics and metabolic instability rendered PD98059 and U0126 unusable in clinical settings (McCubrey et al., 2010).

1.7.2 Inhibitors of MEK for Clinical Use

1.7.2.1 Trametinib

Trametinib (GSK1120212) is an orally bioavailable non-ATP-competitive MEK1/2 inhibitor. Trametinib binds to unphosphorylated MEK1 and MEK2 and prevents phosphorylation induced by RAF (Grimaldi et al., 2017). In phase 3 clinical trials, Trametinib showed significant anti-tumor efficacy in patients with BRAF-mutated melanoma (Flaherty et al., 2012). Trametinib was approved by the United States Food and Drug Administration (FDA) in 2013 to treat BRAF-mutated melanoma patients.

1.7.2.2 Selumetinib

Selumetinib is a selective, non-ATP-competitive inhibitor of MEK1 and MEK2. Selumetinib treatment showed anti-tumor activity against BRAF and NRAS mutant models, including pancreatic, lung, colon, breast, and hepatocellular carcinoma (Luke et al., 2014). In addition, Selumetinib was effective in treating patients with low-grade ovary and biliary cancer in phase 2 clinical trials (Zhao & Adjei., 2014). The FDA approved Selumetinib in 2020 to treat patients with neurofibromatosis type 1 (NF1) (U.S. Food and Drug Administration, 2020).

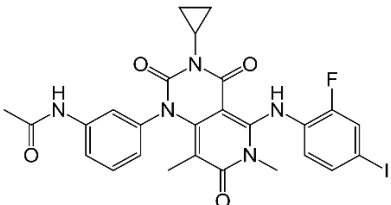
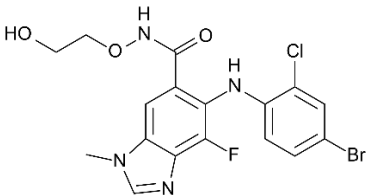
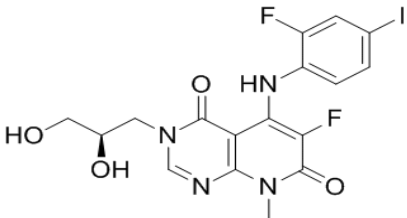
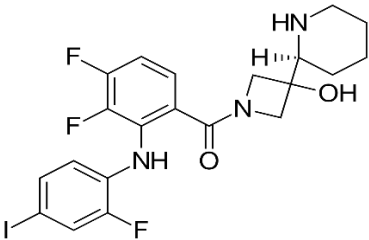
1.7.2.3 Cobimetinib

Cobimetinib is a highly specific, allosteric non-ATP-competitive inhibitor of MEK1 and MEK2. Cobimetinib treatment inhibits the MEK pathway in brain tumors (Zhao & Adjei, 2014). In addition, Cobimetinib treatment inhibited the growth of colon and melanoma tumors with BRAF mutations in human xenograft models (Grimaldi et al., 2017). In 2015, the FDA approved Cobimetinib for clinical uses in combination with Vemurafenib, the Raf inhibitor, to treat advanced melanoma with a BRAF mutation. Cobimetinib is currently being evaluated in phase 2 clinical trial for its safety and efficacy in BRAFV600 melanoma patients with nervous system metastases.

1.7.2.4 Tak733

Tak733 is a selective, non-ATP-competitive allosteric MEK1 and MEK2 inhibitor. Tak733 treatment has broad antitumor activity against multiple cancer cell lines and xenograft models of human melanoma, leukemia, colorectal, pancreatic, and breast cancer (Dong et al., 2011). Phase I study of TAK733 showed anti-tumor effects in patients with BRAF-mutant melanoma without causing significant side effects. However, the anti tumor effects of Tak733 in the study were noted to be limited. (Adjei et al., 2017).

Table 2: MEK inhibitors used in the study.

MEK Inhibitor	Chemical Structure	Clinical status	References
Trametinib		Approved by FDA in 2013 to treat BRAF-mutated melanoma patients.	(Neuzillet et al., 2014)
Selumetinib		Approved by FDA in 2020 to treat patients with neurofibromatosis type 1 (NF1).	(Zhao & Adjei, 2014)
Tak733		Completed phase I clinical trials.	(Adjei et al., 2017)
Cobimetinib		FDA Approved by FDA in 2015, in combination with Vemurafenib to treat advanced melanoma with a BRAF mutation.	(Zhao & Adjei, 2014)
U0126		Not approved for clinical studies. Widely used for basic research	(Cheng & Tian, 2017)

1.7.3 The Ras/MEK Pathway and PpIX Accumulation

A previous study by our laboratory demonstrated that inhibition of the Ras/MEK pathway promotes PpIX accumulation in cancer cells treated with 5-ALA (Yoshioka et al., 2018). Importantly, the promotion of PpIX accumulation by MEK inhibition was cancer specific as MEK inhibition did not increase PpIX accumulation in normal cell lines *in vitro* or in normal tissues *in vivo*. We further identified that MEK inhibition increases PpIX accumulation by targeting two independent pathways (Chelakkot et al., 2020). Hypoxia-inducible factor 1 (HIF-1) is a downstream element of MEK, which activates FECH to convert PpIX to heme. Therefore, MEK inhibition reduces FECH-mediated PpIX conversion to heme, which increases PpIX accumulation. The other pathway is PpIX efflux through ABCB1 regulated by p90 ribosomal S6 kinases (RSKs). RSKs are direct downstream elements of ERKs, which is essential to maintain the expression of ABCB1. Thus, MEK inhibition decreases ABCB1 expression and subsequently reduces PpIX efflux, promoting PpIX accumulation. Figure 4 (Chelakkot et al., 2020) illustrates how MEK inhibition enhances PpIX accumulation in cancer cells.

These findings suggest that using MEK inhibitors during 5-ALA FGS can be a potential strategy to selectively increase PpIX fluorescence in cancer tissue and result in the more sensitive tracing of tumor cells and thus improve the efficacy of FGS.

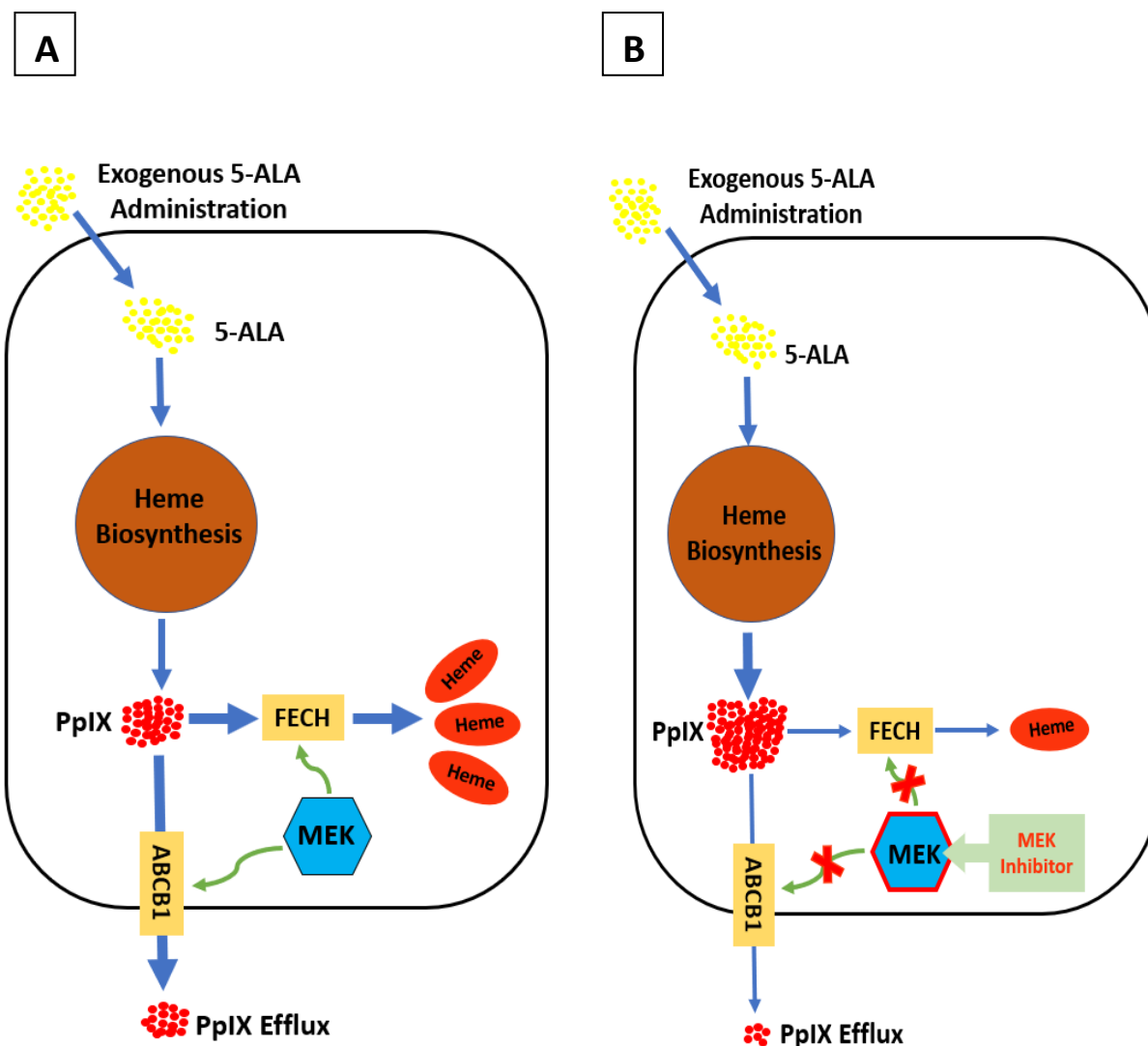


Figure 4: Schematic diagram illustrating the cellular mechanisms involved in elevating cellular PpIX Level by MEK inhibition in a cancer cell.

A. Active MEKs promote FECH activity and ABCB1 expression resulting in increased conversion of PpIX to the heme and PpIX efflux from cancer cells. B. MEK inhibition reduces FECH activity and ABCB1 expression and increases PpIX accumulation in cancer cells.

Note: Adapted from “MEK reduces cancer-specific PpIX accumulation through the RSK-ABCB1 and HIF-1 α -FECH axes” by V.S. Chelakkot, K. Liu, E. Yoshioka, S. Saha, D. Xu, M. Licursi, A. Dorward, and K. Hirasawa, 2020. *Scientific Reports*, 10(1). doi:10.1038/s41598-020-79144-x. [Attribution 4.0 International \(CC BY 4.0\)](https://creativecommons.org/licenses/by/4.0/).

1.8 Study Rationale

The FGS using 5-ALA has been approved for brain tumor removal, leading to improved patient survivability (Stummer, 2006; Polikarpov et al., 2020). However, 5-ALA FGS suffers from multiple shortcomings, including low level or heterogeneous accumulation of PpIX in tumor tissue, resulting in photobleaching and difficulty in the visualization of tumor ends. Thus, our overall research goal is to improve the efficacy of 5-ALA-FGS by selectively enhancing PpIX accumulation in tumors. Previous findings from our lab demonstrated that MEK inhibitor treatment promoted 5-ALA-mediated PpIX accumulation in colon, lung, prostate, and breast cancer cell lines *in vitro* and in mice models of subcutaneous tumor *in vivo* (Yoshioka et al., 2018). The aim of the thesis was to investigate if we observe increased PpIX accumulation in human glioma cell cells by MEK inhibition. Our study aims to use MEK inhibitors that are either clinically approved or are in clinical trials and compare their efficacy in promoting PpIX fluorescence. Additionally, we also aim to establish an experimental system to study PpIX accumulation in brain tumors in mice. If an increase in PpIX accumulation is observed in our study, 5-ALA FGS combined with MEK inhibitors can serve as a strategy to improve the efficacy of tumor removal and patient survival.

Hypothesis and Objective:

I hypothesized that MEK inhibition increases PpIX accumulation in human glioma cells treated with 5-ALA *in vitro*. Moreover, systemic treatment of a MEK inhibitor improves the visualization of brain tumors by 5-ALA-FGS *in vivo*.

To test these hypotheses, 1) We screened different MEK inhibitors for their abilities to promote 5-ALA-mediated PpIX accumulation in human glioma cell lines *in vitro*, 2) We established an animal model of brain tumors, and 3) We evaluated 5-ALA-mediated PpIX accumulation in brain tumors by histological analysis and 2-Photon microscopy.

Chapter 2: Materials and Method

2.1 Cell Culture

This study investigated a panel of human glioma cell lines and one mouse mammary breast cancer cell line. The human glioma cell lines used in this study include SNB75, U343, and SF539 (Table 3), which were obtained from the American Type Culture Collection (ATCC; Manassas, VA, USA). The 4T1 mouse mammary carcinoma cell line was obtained from Dr. Jean Marshall (Dalhousie University). A Luciferase/GFP dual-labeled 4T1 mouse mammary carcinoma cell line was obtained from Genecopoeia (Cat No. 020, Rockville, MD, USA). All cell lines used in this study were maintained in high glucose Dulbecco's modified Eagle's medium (DMEM) (Invitrogen, 11965-118 Canada), supplemented with 10% fetal bovine serum (FBS) (Invitrogen, 12483020, Canada), 1 mM sodium pyruvate (Thermo Fisher Scientific, 11360070, Canada) and antibiotic-antimycotic mixture (Invitrogen, 15240062, Canada) (100 Units/ml penicillin G sodium) in a humidified atmosphere with 5 % CO₂ and 37 °C.

Table 3: Cancer cell lines

Cancer cell Lines	Species affecting	Origin	Cancer subtype	Cell plating density (cells/well)	Reference
SNB75	Human	Brain	Glioblastoma	75x10 ³	(Kishi et al., 2006)
U343	Human	Brain	Glioblastoma	75x10 ³	(Maletínská et al., 2000)
SF539	Human	Brain	Gliosarcoma	75x10 ³	(Rutka et al., 1986)
4T1	Mice (Balb/c)	Mammary Gland	Adenocarcinoma	75x10 ³	(Pulaski et al. 2000)
Luciferase/GFP expressing 4T1	Mice (Balb/c)	Mammary Gland	Adenocarcinoma	-	-

2.2 Reagents

2.2.1 MEK Inhibitors and Their Administration Protocol

MEK inhibitor U0126 was purchased from Cell Signaling Technology (Danvers, USA) and Selumetinib, Binimetinib, Cobimetinib, Trametinib, and Tak733 (Table 2) from Selleckchem (Huston, TX). These MEK inhibitors were dissolved in DMSO (Sigma, D2650, USA) at a stock concentration of 5 mM. The stock solution was kept at -80 °C, prepared as single thaw aliquots for immediate experimental use. For *in vitro* studies, cultured cells were treated with one of the listed MEK inhibitors or DMSO as a diluent control at equivalent percentages to the MEK inhibitor stock.

2.2.2 5-ALA and its Administration Protocol

5-ALA was purchased from Sigma (Oakville, ON). For *in vitro* studies, monolayer cells were treated with 5-ALA prepared as a sterile stock in serum-free Dulbecco's Modified Eagle Medium (DMEM) (Invitrogen, Ontario, Canada). The 5-ALA stock solution (125 mM) was aliquoted in small volumes and kept at -80 °C with immediate experimental use after a single freeze-thaw cycle.

2.3 Quantification of PpIX Accumulation *in vitro*

Cells were plated in 24 well plates at the density of 75×10^3 cells/well, suspended in 500 μ l of medium. The plates were then incubated overnight to reach 70-80 % confluence. The medium was then replaced with a fresh 500 μ l medium containing either a MEK inhibitor or DMSO (1%) as vehicle control for 24 h. 5-ALA was added to the wells 4 h before sampling at a final

concentration of 5 mM. The incubation timepoints, and 5-ALA concentrations were based on our previous publications (Chelakkot et al., 2019; Yoshioka et al., 2018). At the end of MEK inhibitor and 5-ALA treatment, cells were lysed with 100 μ l of radioimmunoprecipitation assay (RIPA) buffer (PBS pH 7.4, NP-40 1% (Sigma, USA), 0.1% sodium dodecyl sulfate (SDS) (Bio-Rad, Canada) and 0.5 % sodium deoxycholate (Sigma, USA). The cell lysates were centrifuged at 11,000 x g for 10 min at 4 °C. The supernatant was transferred to a clean tube and stored at -80 °C. Cell lysates were diluted (1:20) in PBS, and 200 μ l of the diluted cell lysates were loaded in a 96 well plate. PpIX fluorescence was measured using a Synergy Mx 4 Fluorescence plate reader (BioTek Instruments Inc. VT) with a 405 nm excitation/630 nm emission filter.

2.4 Western Blot

Following the treatment with the indicated reagents, cells were lysed with 100 μ l of radioimmunoprecipitation assay (RIPA) buffer containing phenylmethylsulfonyl fluoride (PMSF) (Sigma-Aldrich, Missouri), aprotinin (Sigma-Aldrich), and phosphatase inhibitors (halt phosphatase inhibitor cocktail, Thermo Fisher Scientific) in a 1:2:1 ratio respectively. The total cell lysate (TCL) was mixed with 3X Bromophenol Blue (BPB) loading dye in a 1:2 ratio by volume, and the resulting mixtures were boiled at 100 °C for 5 min. 7 μ l of protein samples were loaded onto 4 to 12% gradient sodium dodecyl sulfate-polyacrylamide gel electrophoresis (SDS-PAGE) gels and run (Bio-Rad, ON, Canada) at a constant current of 20 mA for 1 h. The separated proteins were transferred onto 0.2 μ m nitrocellulose membranes (Bio-Rad, ON, Canada) using a Tran-blot Turbo Transfer System (Bio-Rad) for 7 min and blocked with 5% skim milk in tris-buffered saline with tween 20 (TBST) buffer for 1 hr. The membranes were then probed with appropriate primary antibodies in conditions shown in Table 3 overnight at 4°C. The following day, the membranes were washed three times with TBST, followed by incubation with horseradish

peroxidase (HRP) conjugated secondary antibodies (anti-mouse IgG or anti-rabbit IgG) (Santa Cruz Biotechnology) in conditions shown in Table 4 for 1 hour at room temperature. Protein was detected by chemiluminescence, using substrates (RPN2235, GE healthcare, Italy; Bio-Rad, Canada) and ImageQuant LAS 4000 image analyzer (GE Healthcare, Buckinghamshire, UK).

Table 4: Primary and secondary antibody conditions for western blot

Antibody	Primary antibody condition	Secondary antibody condition
pERK1/2 Thr202/Thr204 (Cell Signalling 9101S)	1:1,000 in 5 % skim milk in TBST	1:5000 Anti-rabbit IgG in TBST
ERK 1 antibody (K-23) (Santa Cruz SC-94)	1:30,000 in 5% skim milk in TBST	1:5000 Anti-rabbit IgG in TBST
GAPDH (Abcam 6C5)	1:500,000 in TBST	1:5000 Anti-mouse IgG in TBST

2.5 Animal Studies

2.5.1 Mice Strains

Balb/c female mice, 4 weeks old, were obtained from Charles River Labs (Montreal, Canada). All mice were housed in isolated ventilated caging units with Bed-O-Cobs bedding (The Andersons Inc, Maumee, OH) and suitable enrichment; cages were kept in the animal care facility at the Health Sciences Centre at Memorial University of Newfoundland. All animal experiments followed the animal care protocols approved by the Institutional Animal Care Committee, in accordance with Canadian Council on Animal Care guidelines. Mice were fed with Laboratory Rodent Diet 5010 (27.5 % protein, 13.5 % fat, 59 % carbohydrate; OM Nutrition International, Richmond, IN) with water ad libitum and were housed individually under a 12:12 hour light/dark cycle.

2.5.2 Mice Allograft Model

For this study, we developed a luciferase/GFP dual-labeled 4T1 mice mammary carcinoma cell allograft model in mice brains. First, 4T1 cells expressing luciferase/GFP were grown as a monolayer in a 10 cm culture dish. Upon reaching confluency, cells were trypsinized and washed 3x in PBS, followed by resuspension in saline to reach a concentration of 10×10^5 cells/100 μ l. To inoculate the cells, female Balb/c mice of age 8 weeks were anesthetized using isoflurane, positioned in a stereotactic device using ear bars and injected with buprenorphine (5 mg/Kg). An incision was made to the skin to expose the skull, and a small burr hole was drilled through the skull at 1.0 mm anterior and 1.0 mm lateral to the bregma. A 20-gauge needle (Hamilton Company, USA) was inserted to a depth of 3.0 mm from the skull surface to inject 3×10^5 cells suspended in

3 μ l ice-chilled saline. Following the surgery, survival and well being of animals were monitored daily.

2.5.3 PpIX Fluorescence Imaging

After an incubation period of 10-12 days, the mice with established brain tumors were injected intraperitoneally (i.p) with 5-ALA (200 mg/kg body weight (BW)) prepared in 200 μ L sterile saline (0.85% NaCl, Hospira, Canada) at 2 hours prior to sacrifice. Animals were moved to a dark room to prevent any 5-ALA induced photosensitivity until sacrifice. Brain tissue samples were collected from all the animals following euthanasia in CO₂. For epifluorescence imaging of brain tumors, collected brain sections were flash-frozen, embedded in optimum cutting temperature (OCT) compound (Thermo Fisher Scientific, Canada), and stored at -80 C°. The site of a tumor in the brain samples was identified, and serial coronal sections of 20 μ m thickness were mounted on glass slides (Leica, IL, USA). These coronal sections with tumor were imaged using Carl Zeiss Axio Scan.Z1 Digital Slide Scanner, fitted with a 635 nm emission lens filter. White light was used for bright field imaging, and blue light (405 nm) was used for PpIX fluorescence imaging. Precautions were taken to limit the exposure of the sections to light in consideration of the photosensitivity of PpIX and its decay in bright light.

For 2-Photon microscopy, the mice with established brain tumors, after an incubation period of 10-12 days, received Selumetinib orally (150 mg/kg BW in 100 μ l of phosphate buffered saline (PBS)), or control vehicle (0.5% propyl methyl cellulose in PBS) at 4 hours prior to sacrifice. All the mice received i.p. 5-ALA (200 mg/kg BW in 200 μ L saline) at 2 hours prior to sacrifice. Animals were moved to a dark room to prevent any 5-ALA induced photosensitivity until sacrifice. The mice were anesthetized by isoflurane inhalation, and the brains were removed. The collected

mice brains were placed in ice-cold slicing solution, and thick coronal sections (350 μ m) were obtained using a vibratome (Leica, IL, USA). The 2-Photon microscope is fitted with Gallium arsenide phosphide (GaAsP) photomultiplier tubes (PMTs) to detect light. To excite the fluorophore, a laser of 800 nm wavelength, generated by Chameleon Vision II (Coherent) was used. The microscope was not fitted with an excitation filter as the laser source was tuned to 800 nm. Once the fluorophores were excited, fluorescence emission was collected using a Nikon 16x/0.8 NA water-immersion objective, and a 620/60 nm bandpass filter directed the PpIX emission to the PMT, where the fluorescence signal was detected. The coronal sections were imaged in artificial cerebrospinal fluid (ACSF) (Barnes et al., 2020). We used galvo-galvo scanning mirrors to scan images at a resolution of 2048 x 2048 pixels. Z-stacks were collected using a 1-micron step interval. Images were acquired using Scanimage Premium Software (Vidrio Technologies, VA, USA) according to a published protocol.

2.6 Statistical Analysis

One-way ANOVA with Dunnett's post-hoc test was performed using GraphPad Prism 8.0c software (GraphPad Software, La Jolla, CA, USA) to compare multiple groups. $P < 0.01$ was considered statistically significant.

Chapter 3: Results

3.1 Screening of Different MEK Inhibitors Promoting PpIX Accumulation:

To determine which MEK inhibitors could promote the accumulation of PpIX fluorescence, we tested 4 MEK inhibitors Trametinib, Tak 733, Selumetinib, and Cobimetinib, on human glioma cell lines. In addition, we also used mouse breast cancer 4T1 cells, which form brain tumors in inbred BALB/c mice. MEK inhibitor U0126 was included in each experiment as a positive control because previous studies in our lab showed that U0126 treatment promotes PpIX accumulation in a majority of human cancer cell lines tested (Yoshioka et al., 2018).

3.1.1 SNB75

PpIX accumulation was significantly promoted in human glioma SNB75 cell line by treatment of Trametinib ($p < 0.0001$, one-way ANOVA), Tak733 ($p < 0.0001$, one-way ANOVA), Selumetinib ($p < 0.0001$, one-way ANOVA), or Cobimetinib treatment ($p < 0.0001$, one-way ANOVA) at all the concentrations tested (Figure 5A, 5B, 5C and 5D).

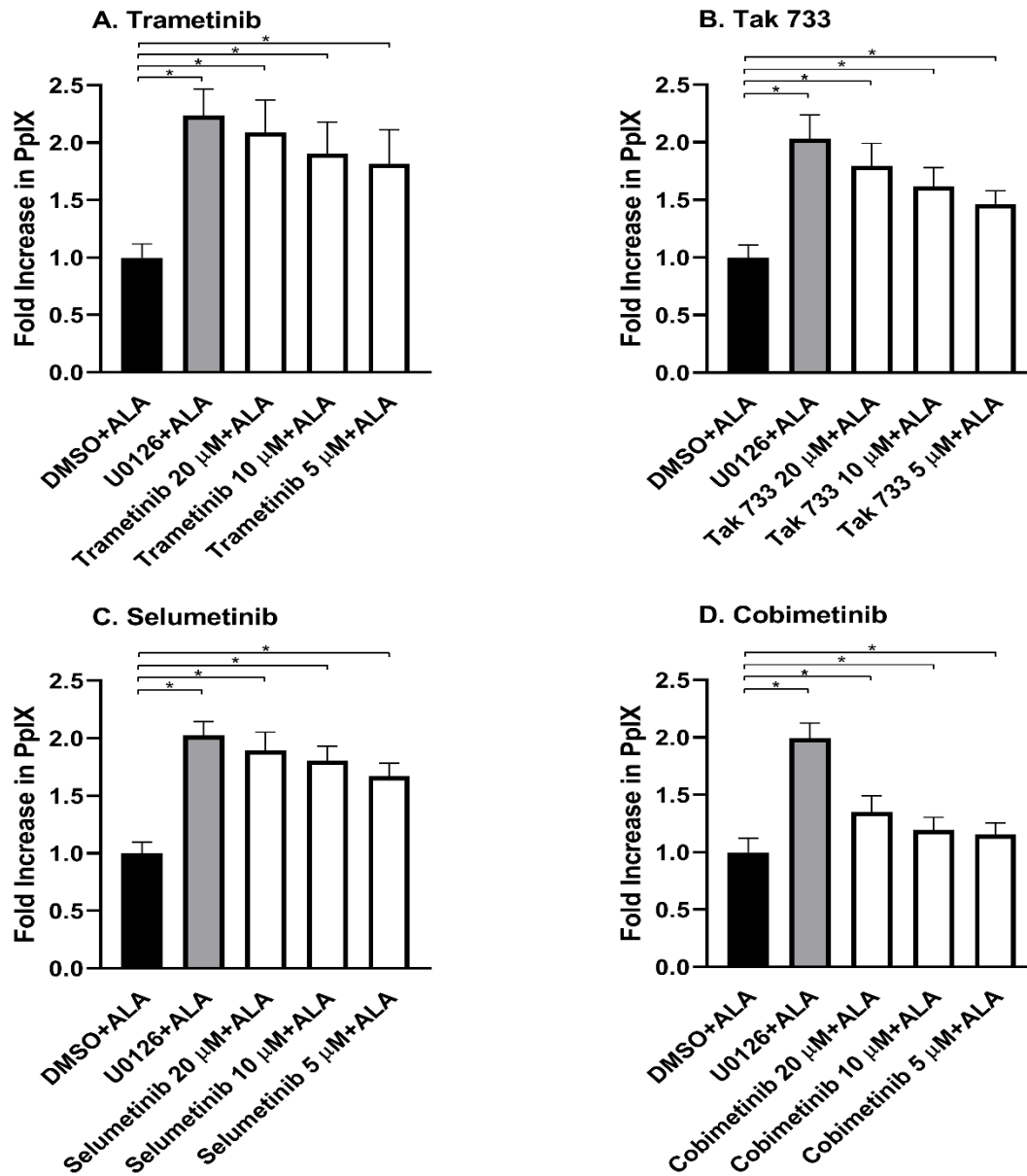


Figure 5: Effect of MEK inhibitors on PpIX accumulation in SNB75 human glioma cell line.

Cells were treated with control vehicle (DMSO), U0126 (20 μ M), or MEK inhibitor ((A) Trametinib (B) Tak733 (C) Selumetinib (D) Cobimetinib) at indicated concentrations for 24 hours and with 5-ALA (5 mM) for 4 hours prior to cell lysis. Cellular PpIX is presented as a fold increase compared with vehicle control DMSO. Plot shows mean \pm SD (standard deviation) of three biological replicates. Statistical analysis was conducted using one-way ANOVA, Dunnett's post test * p <0.01.

3.1.2 SF539

We tested if the MEK inhibitors could promote 5-ALA induced PpIX accumulation in human glioma cell line SF539. No significant increase in PpIX accumulation was noted in cells treated with any MEK inhibitors (Trametinib ($p=0.1999$, one-way ANOVA), Tak733 ($p=0.1781$, one-way ANOVA), Selumetinib ($p=0.3204$, one-way ANOVA), Cobimetinib ($p=0.2931$, one-way ANOVA)) including the positive control U0126 (Figure 6). This result suggested that PpIX accumulation in SF539 cells is not sensitive to MEK inhibition.

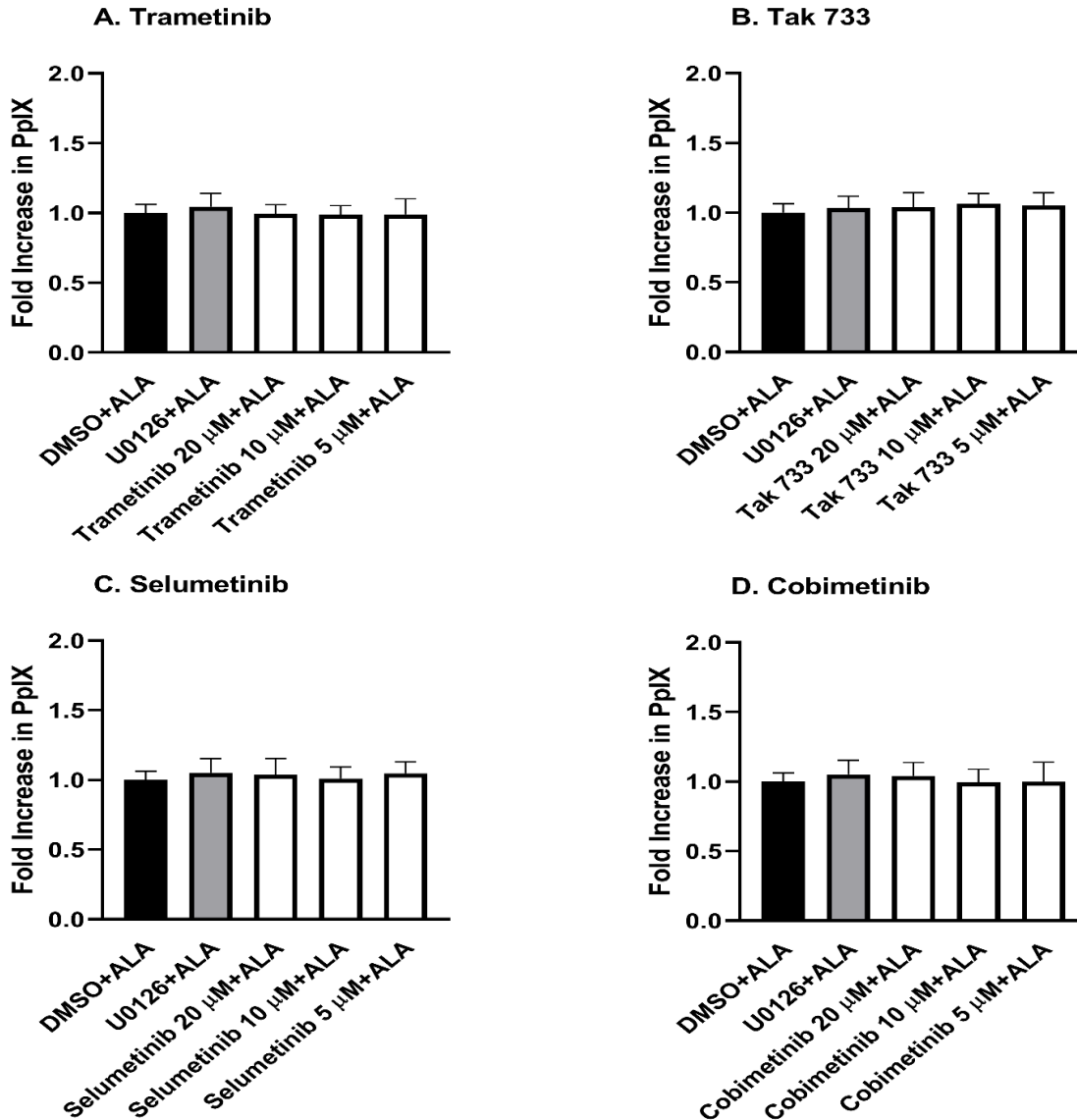


Figure 6: Effect of MEK inhibitors on the PpIX accumulation in SF539 human glioma cell line.

Cells were treated with control vehicle (DMSO), U0126 (20 μ M), or MEK inhibitor ((A) Trametinib (B) Tak733 (C) Selumetinib (D) Cobimetinib) at indicated concentrations for 24 hours and with 5-ALA (5 mM) for 4 hours prior to cell lysis. Cellular PpIX is presented as a fold increase compared with vehicle control DMSO. Plot shows mean \pm SD (standard deviation) of three biological replicates. Statistical analysis was conducted using one-way ANOVA.

3.1.3 U343

We examined if the MEK inhibitors promote 5-ALA-induced PpIX accumulation in human glioma cell line U343. PpIX accumulation was significantly increased by treatment with Trametinib ($p < 0.0001$, one-way ANOVA), TAK733 ($p < 0.0001$, one-way ANOVA), or Selumetinib ($p < 0.0001$, one-way ANOVA) at all the concentrations we tested (Figure 7A, 7B and 7C). In contrast, Cobimetinib treatment ($p < 0.0001$, one-way ANOVA) did not increase PpIX accumulation at any of the concentrations tested (Figure 7D). Meanwhile, the U0126 treatment (positive control) significantly promoted PpIX accumulation in the same experiment, suggesting that Cobimetinib is not effective in increasing the PpIX accumulation in U343.

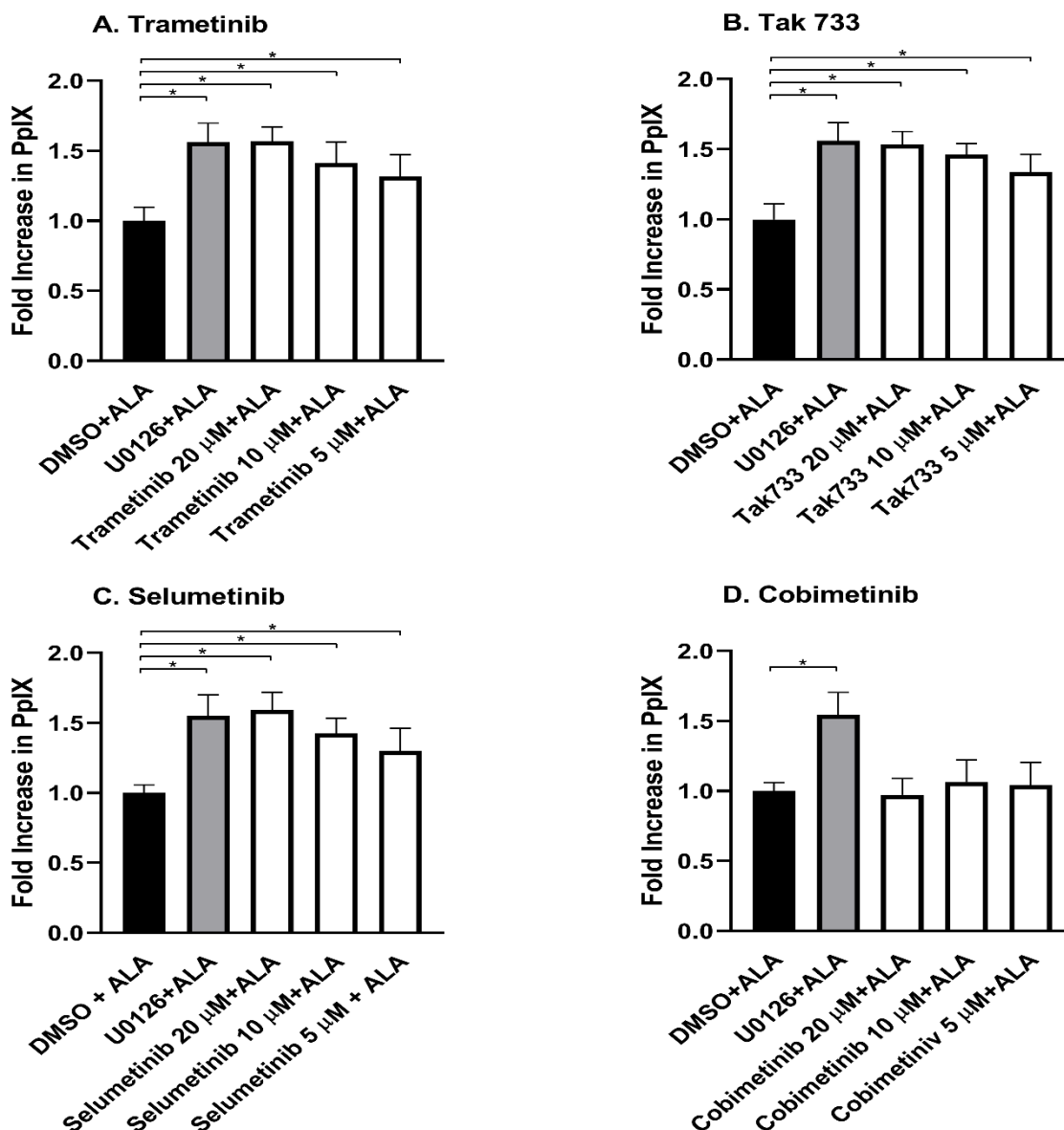


Figure 7: Effect of MEK inhibitors on the PpIX accumulation in U343 human glioma cell line.

Cells were treated with control vehicle (DMSO), U0126 (20 μ M), or MEK inhibitor ((A) Trametinib (B) Tak733 (C) Selumetinib (D) Cobimetinib) at indicated concentrations for 24 hours and with 5-ALA (5 mM) for 4 hours prior to cell lysis. Cellular PpIX is presented as a fold increase compared with vehicle control DMSO. Plot shows mean \pm SD (standard deviation) of three biological replicates. Statistical analysis was conducted using one-way ANOVA, Dunnett's post test * p <0.01.

3.1.4 4T1

Given that the brain is one of the target organs of breast cancer metastasis, we examined the efficacy of the MEK inhibitors on 5-ALA-induced PpIX accumulation in mouse mammary cancer 4T1 cell line. We selected 4T1 cells as they form brain tumors in inbred BALB/c mice, and unpublished observations from our lab show that 4T1 cells are most sensitive to PpIX upregulation mediated by MEK inhibition among a panel of murine cancer cell lines. Moreover, the 4T1 brain tumor model was an efficient model system for us to optimize *in vivo* experiments compared to using immune compromised mice bearing tumors originating from human cancer cell lines. It also gave us an opportunity to test the efficacy of MEK inhibitor treatment in an immune competent *in vivo* model.

For this *in-vitro* experiment, we used broader ranges of the drug concentration (Trametinib (20 μ M, 10 μ M, 5 μ M, 1 μ M, 500 nM and 250 nM), Tak733 (20 μ M, 10 μ M, 5 μ M, 1 μ M, 500 nM and 250 nM), Selumetinib (20 μ M, 10 μ M, 5 μ M, 1 μ M, 500 nM and 250 nM) and Cobimetinib (20 μ M, 10 μ M, 5 μ M, 1 μ M, 500 nM and 250 nM)). PpIX accumulation was significantly promoted in 4T1 cells by treatment with Trametinib ($p < 0.0001$, one-way ANOVA), Tak733 ($p < 0.0001$, one-way ANOVA), or Cobimetinib ($p < 0.0001$, one-way ANOVA) at all the concentrations we tested (Figure 8A, 8B, and 8D), but we failed to see any dose-response pattern with the application of these MEK inhibitors. MEK inhibition by Selumetinib ($p < 0.0001$, one-way ANOVA) also resulted in the promotion of PpIX accumulation at higher concentrations of 20 μ M, 10 μ M, and 5 μ M but not at lower concentrations of 1 μ M, 500 nM, and 250 nM (Figure 8C). In addition, we observed a dose-response pattern in PpIX accumulation with Selumetinib treatment. To determine whether the MEK inhibitors were effective in inhibiting the MEK pathway, we performed western blot analysis using antibodies against phosphorylated ERK (p-ERK), total ERK

(t-ERK), and GAPDH. As ERKs are the direct downstream elements of MEK, inhibition of MEK activity is expected to reduce the phosphorylation levels of ERKs. As shown in Figures 9A, 9B, and 9D, p-ERK was not detected in 4T1 cells treated with Trametinib, Tak733, or Cobimetinib at all the concentrations tested. Similarly, Selumetinib treatment inhibited the MEK pathway completely at higher concentrations (20 μ M, 10 μ M, and 5 μ M) (Figure 9C). Overall, all the inhibitor treatments were effective in inhibiting the activation of the MEK pathway. Moreover, the expression levels of GAPDH were not reduced by the treatments of the inhibitors, suggesting that the drug concentrations used in the experiments did not affect cell viability and metabolism.

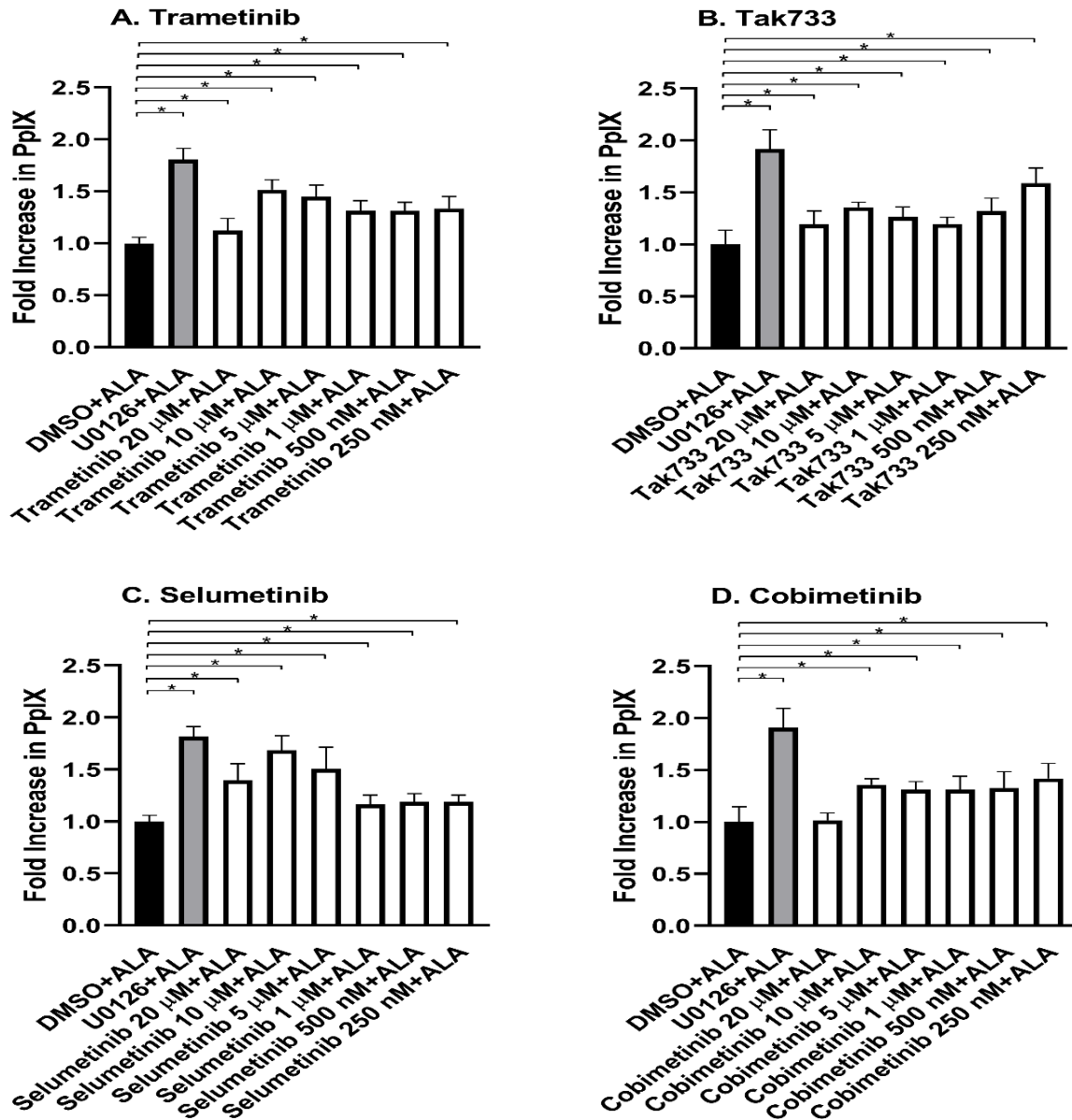


Figure 8: Effect of MEK inhibitors on the PpIX accumulation in 4T1 mice mammary cancer cell line.

Cells were treated with control vehicle (DMSO), U0126 (20 μ M), or MEK inhibitor ((A) Trametinib (B) Tak733 (C) Selumetinib (D) Cobimetinib) at indicated concentrations for 24 hours and with 5-ALA (5 mM) for 4 hours prior to cell lysis. Cellular PpIX is presented as a fold increase compared with vehicle control DMSO. Plot shows mean \pm SD (standard deviation) of three biological replicates. Statistical analysis was conducted using one-way ANOVA, Dunnett's post test * p <0.01.

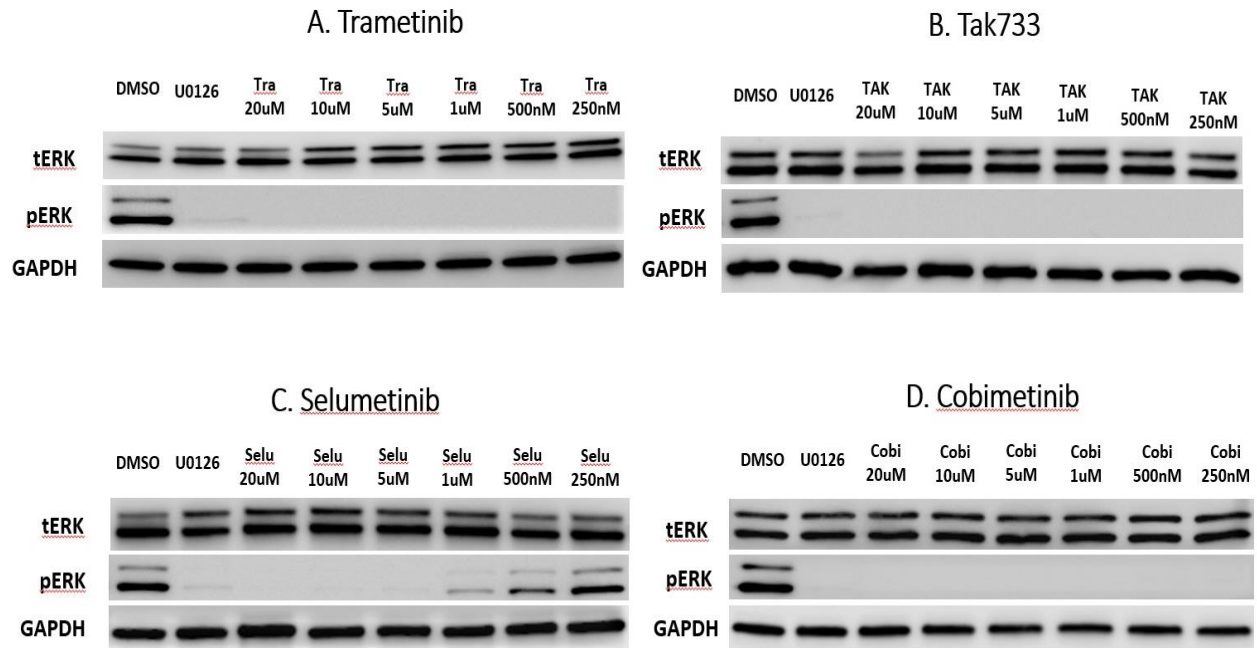


Figure 9: MEK Inhibition resulted in reduced ERK phosphorylation in mouse mammary cancer 4T1 Cell line.

4T1 cells were treated with DMSO (vehicle control), U0126 (20µM) or MEK inhibitors (A) Trametinib (B) Tak733 (C) Selumetinib and (D) Cobimetinib) at concentrations of 20µM, 10µM, 5µM, 1µM, 500nM and 250nM for 20 hours. Western blot was conducted using antibodies against total ERK (t-ERK), phosphorylated ERK (pERK), and GAPDH.

3.2 Effect of MEK Inhibition on PpIX Accumulation *in vivo*.

3.2.1 Establishment of an Animal Model of Brain Tumor

Our long-term goal is to determine if systemic treatment of a MEK inhibitor promotes cancer specific PpIX fluorescence in *in vivo* brain tumors. As the first step, we sought to develop a luciferase/GFP dual-labeled 4T1 allograft model of brain tumors using Balb/c mice (Figure 10 A). As seen in Figure 10B, brain tumors were developed by injecting 4T1 cells expressing GFP (3×10^5 cells/3 ml) intracranially in the right hemisphere of the brain. At 10-12 days after surgery (Figure 10C), the mice received an i.p. injection of 5-ALA (5 mM) and 2 hours later euthanized in CO₂. The presence of brain tumors was confirmed under white light (Figure 10D) and under blue light (Figure 10E), which shows cancer-specific pink fluorescence of PpIX. The brain was then embedded in OCT and flash frozen in dry ice (Figure 10F). Serial coronal sections of 20 μm thickness were prepared from the frozen tissue samples and mounted on glass slides (Figure 10G). Some of these sections were stained with hematoxylin and eosin (H&E) staining to confirm tumors in the brain (Figure 11H).

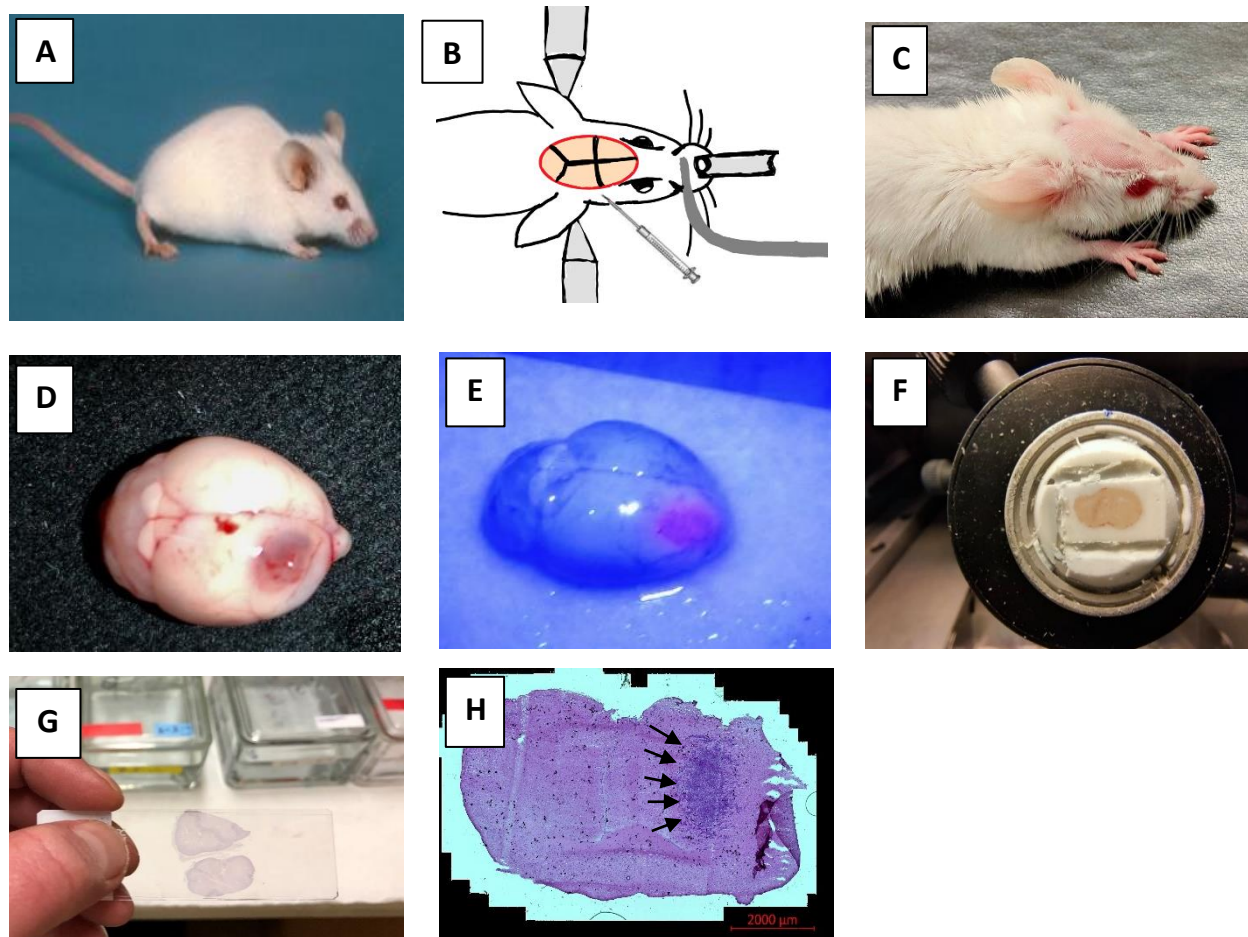


Figure 10: Generation of an animal model of a brain tumor in Balb/c mice strain.

(A) For *in vivo* studies, a 4T1 brain tumor model was generated in the Balb/c mice strain. (B) Intracranial injection of GFP-expressing 4T1 cells into the right hemisphere of the brain. (C) Mice with a developed tumor in the brain 12 days post injection. Extracted brains with tumors were visualized (D) under white light and blue light (E). (F) Sectioning of flash-frozen brain sample embedded in OCT. (G and H) Coronal sections of the brain (20 μm) mounted on a glass slide were stained with H&E to confirm the location of tumors (black arrows) (Scale bar reflects 2000 μm).

3.3 Establishing Protocol for Fluorescence Microscopy

The brain sections were visualized using Zeiss Axio scan Z1 high throughput slide scanner for PpIX and GFP fluorescence. As we used luciferase/GFP-expressing 4T1 cells for the *in vivo* experiments, GFP fluorescence demonstrates the location of brain tumors. As shown in Figure 11A, GFP fluorescence was observed in the right hemisphere of the brain, indicating that the tumor was developed at the injection site of 4T1 cells. The GFP fluorescence signal was stronger at the edge of the tumor, with diffuse fluorescence throughout the other tumor areas. Additionally, the red fluorescence of PpIX was also observed at the same region of the brain, but not outside of tumor areas (GFP) positive, suggesting tumor specific accumulation of PpIX in the brain tumor (Fig 11B). Moreover, when GFP and PpIX fluorescence were compared, they mostly overlapped (Fig 11C). However, the PpIX fluorescence contrast between normal and tumor tissue was insufficient to generate a sharp delineation of tumor ends.

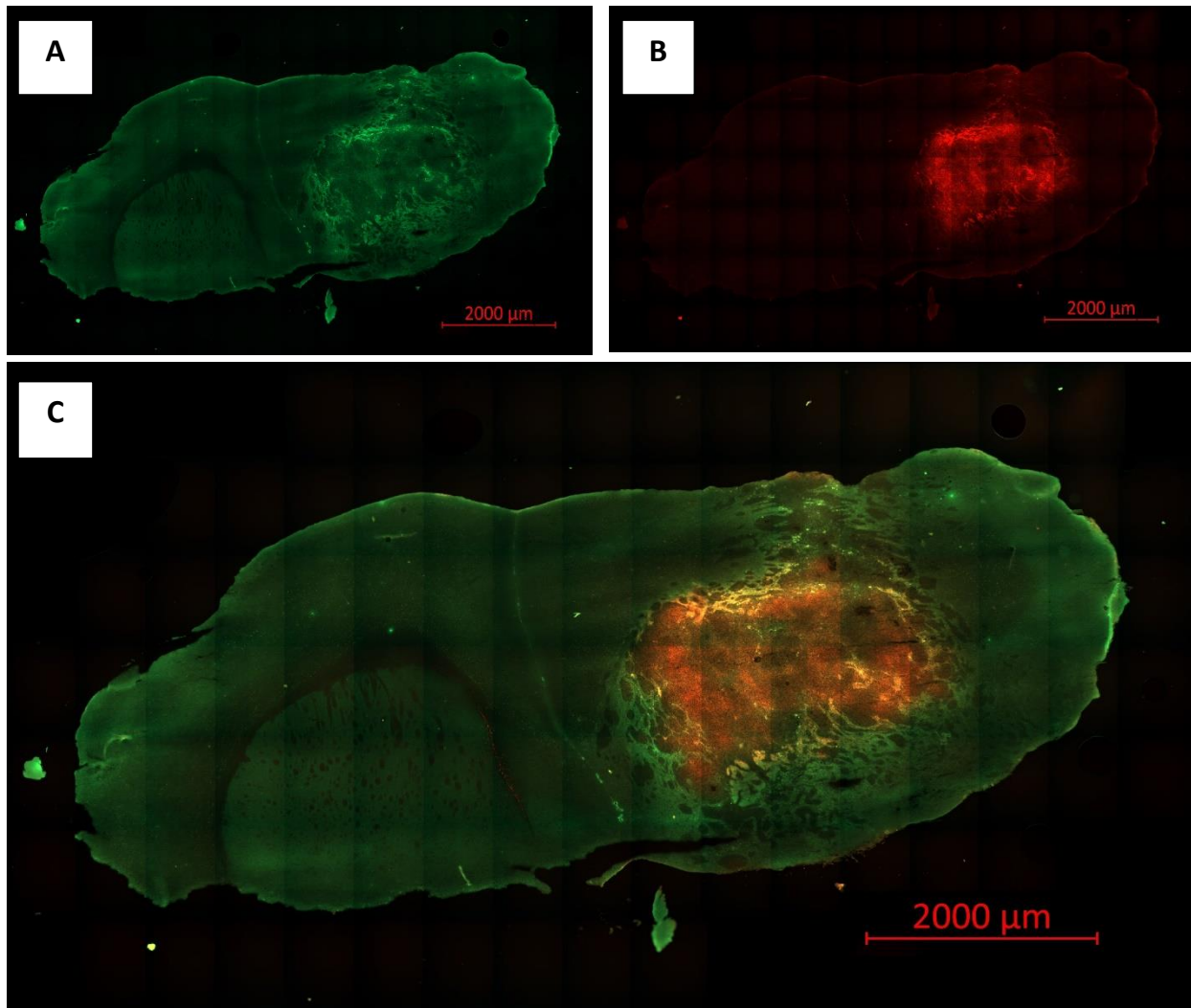


Figure 11: Visualisation of brain tumor fluorescence *in vivo*.

Fluorescence images of GFP-expressing 4T1 tumors in the brain were obtained from BALB/c mice treated with 5-ALA (200 mg/kg BW) at 2 hours prior to sacrifice. (A) GFP fluorescence and (B) PpIX fluorescence images were taken on the coronal section of the mice's brain with a tumor. (C) Overlay image of PpIX channel over GFP channel. Fluorescent images were taken on brain samples from a minimum of three different mice. The images represent brain sample from one of the mice.

3.4 Tumor Imaging Using 2-Photon Microscopy

We investigated if 2-Photon microscopy analysis can be used as another approach to evaluating PpIX fluorescence of tumors in the brain. Here, we also conducted preliminary experiments to determine the efficacy of *in vivo* MEK inhibitor treatment on PpIX fluorescence in brain tumors. For this experiment, we decided to use Selumetinib as the MEK inhibitor as it showed a consistent and high degree promotion of PpIX accumulation in *in vitro* experiments (Figure 5C, 7C, and 8C). Selumetinib is also a well-established inhibitor of MEK in animal models of cancer (Bartholomeusz et al., 2012; Ryu et al., 2017).

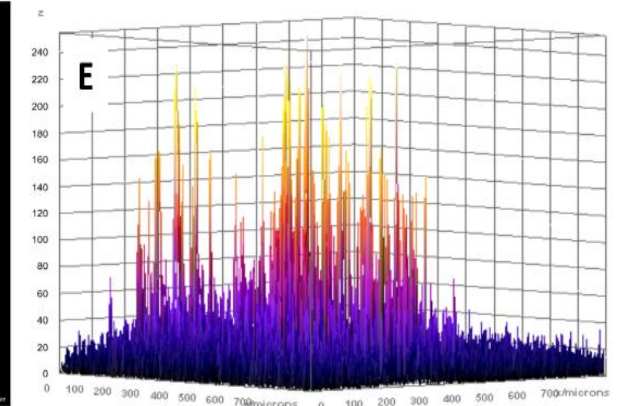
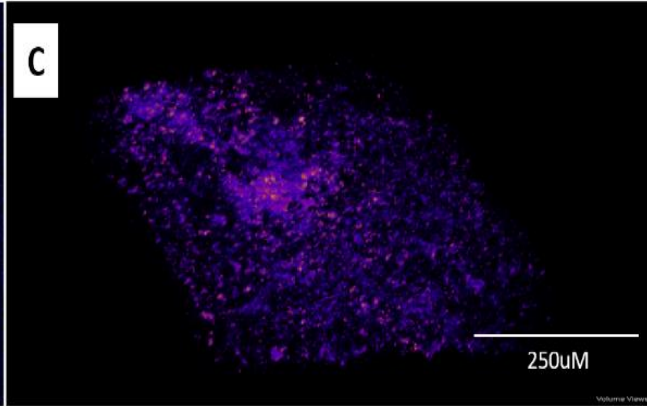
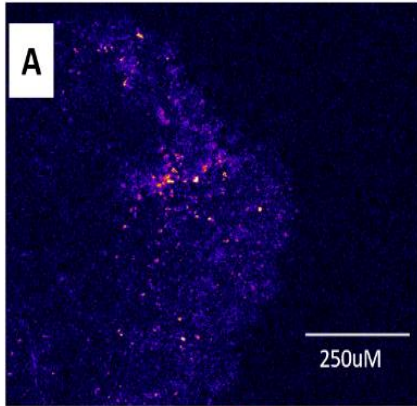
The *ex vivo* 2-Photon microscopy analysis showed the promotion of PpIX accumulation in brain tumors of mice treated with Selumetinib (Figure 12), consistent with the results we observed in *in vitro* studies (Figure. 8C). In addition, we found that the fluorescence distribution across the tumor tissue was more homogenous and the fluorescence contrast between the tumor and adjacent healthy tissue was more pronounced, resulting in clear visualization of tumor ends. Although the experiments are still preliminary, they indicate the potential use of the MEK inhibitor treatment to promote cancer specific PpIX fluorescence promotion during brain tumor removal surgery.

Fluorescence intensity

Volume view

3D surface plot

5-ALA



Selu + 5-ALA

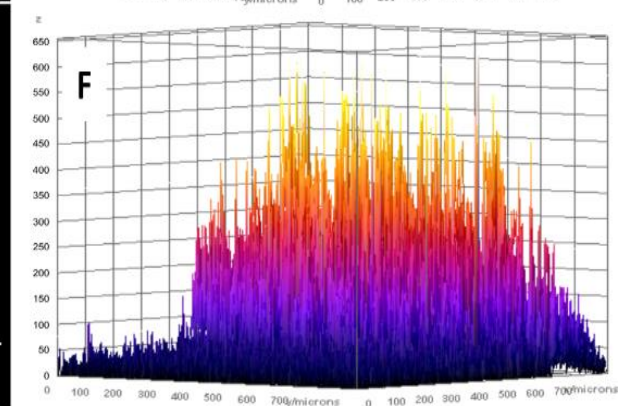
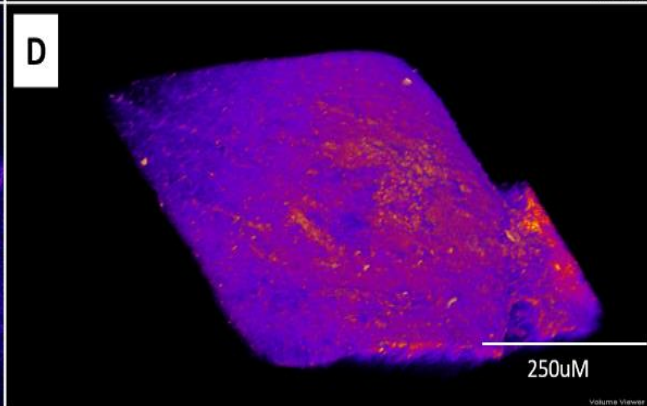
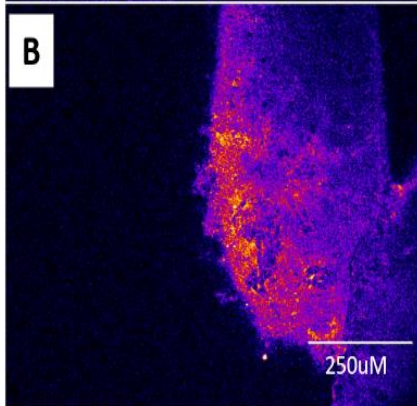


Figure 12: Brain tumor imaging of PpIX fluorescence by 2-Photon microscopy.

Fluorescence images of 4T1 brain tumors obtained from BALB/c mice treated with control vehicle (A, C, and E) and with Selumetinib (250 mg/kg BW) (B, D, and F) for 4 hours, and with 5-ALA (200 mg/kg BW) for 2 hours. (A and B) 2-D Tumor image at a depth of 100 μm into the tissue showing PpIX fluorescence from the control group (A) or experimental group (B). (C and D) A stack of 300 images of the brain slices at a spacing of 1 μm , representing tissue z-axis (volume view) from the control group (C) or experimental group (D). (E and F) 3-D fluorescence intensity map. (E) was generated from images A and C, and (F) generated from images B and D. The color corresponds to the PpIX fluorescence intensity, ranging from blue (low) to red (high).

Chapter 4: Discussion

4.1 *In vitro* Screening of MEK Inhibitors

We identified two candidate MEK inhibitors that may be useful for enhancing PpIX accumulation in tumor cells. To screen for MEK inhibitors capable of promoting PpIX accumulation, a panel of human glioma cell lines was selected and treated with 5-ALA plus various MEK inhibitors at different concentrations. MEK inhibition by Selumetinib increased PpIX accumulation in 2 of 3 glioma cell lines (Figure 5 and 7). Selumetinib treatment also showed the greatest promotion of PpIX accumulation (1.68 fold) in mouse breast cancer 4T1 cells among the MEK inhibitors we tested (Figure 8). Additionally, we observed a dose-dependent increase in PpIX accumulation with Selumetinib treatment. This dose-dependency can be explained by the western blot of phosphorylated ERK in 4T1 cell line (Figure 9), where Selumetinib treatment did not completely inhibit MEK activity at lower concentrations (1 μ M to 250 nM), while at higher concentrations (5 μ M to 20 μ M) we saw a complete inhibition of MEK activity. Moreover, Selumetinib was approved for treating patients with neurofibromatosis type 1 (NF1) by the FDA in 2020 (U.S. Food and Drug Administration, 2020). Based on these, we prioritized Selumetinib as our first MEK inhibitor for further investigation.

Our second candidate is Trametinib, which has been evaluated in multiple clinical trials as an anti-tumor therapeutic and has been approved for treating BRAF mutated melanoma patients (Neuzillet et al., 2014; Falchook et al., 2012; Grimaldi et al., 2017). Trametinib treatment similarly promoted PpIX accumulation in human glioma cell lines (Figure 5 and 7), while it was less effective than Selumetinib in the 4T1 cell line (Figure 8). Given this, and because we used 4T1 allograft brain tumor mice for our *in vivo* studies, we selected Selumetinib in this thesis project to test its efficacy in *in vivo* experiments. The *in vivo* efficacy of Trametinib will be evaluated in the

Hirasawa lab in the future. The selection of MEK inhibitors that are already approved for clinical use, such as Selumetinib and Trametinib, was critical since any improvement in PpIX fluorescence and tumor visualization in our *in vivo* preclinical studies can pave the way for future clinical investigations.

As seen in Figure 8, the use of MEK inhibitor Trametinib and Selumetinib at a concentration of 20 μ M resulted in a decrease in PpIX accumulation in 4T1 cells, compared to lower concentrations. A reason for such observation can be attributed to the effects of MEK inhibitors on cancer cell lines. Several studies indicate that MEK inhibitors in high concentrations may induce cytostatic effects, limiting cell division and growth (Selvasaravanan et al., 2020; Smalley & Flaherty, 2009). Suppression on the proliferation kinetics of the cancer cells, treated with MEK inhibitors, can lower the cellular activity required to generate PpIX from 5-ALA metabolically. However, the western blot from Figure 9 suggests that the drug concentrations did not affect cell viability. In future studies, we can perform MTT assays and metabolic assays to assess cell viability and confirm this further. Another reason can be the blockage of cell membranes and the prevention of endosmosis at a higher concentration of the MEK inhibitors, which is permitted at lower concentrations.

Cobimetinib treatment did not promote PpIX accumulation in U343 and SF539 cell lines (Figure 6 and Figure 7) at any of the concentrations tested. Additionally, the degree of increase in PpIX accumulation with Cobimetinib treatment in SNB75 cell line was lowest among all the MEK inhibitors tested in the study (Figure 5). These results suggest that Cobimetinib is not as effective in promoting PpIX accumulation in human glioma cell lines compared to the other MEK inhibitors we tested, such as Trametinib, Tak733, and Selumetinib. Nevertheless, Cobimetinib successfully promoted PpIX accumulation (Figure 8) and reduced the amount of phosphorylated ERK in 4T1

cells throughout the concentrations tested (Figure 9). To examine why Cobimetinib is not as effective in human glioma cell lines, we will need to compare the phosphorylation levels of ERK in glioma cell lines to those in 4T1 cell line by Western Blot analysis in the future.

The different mechanisms by which the MEK inhibitors used in our study achieve MEK inhibition may explain the disparity in levels of PpIX upregulation observed. Trametinib, Selumetinib, and Tak733 inhibit RAF-dependent phosphorylation of MEK1 on S217 (Luke et al., 2014). In contrast, Cobimetinib binds to phosphorylated MEKs and prevents their binding to the downstream elements, ERKs (Spain et al., 2016). These mechanisms of action may contribute to the different effects of Cobimetinib on PpIX accumulation in the glioma cell lines. Alternatively, MEK inhibition downregulates ABCB1 expression and FECH activity to promote PpIX accumulation (Yoshioka et al., 2018). Therefore, any off-target effects of Cobimetinib treatment directly regulating the activity of FECH and ABCB1 can negate the effect of MEK inhibition on PpIX accumulation. To address these questions, a Western Blot analysis to measure the effects of Cobimetinib treatment on activity levels of FECH and ABCB1 expression can be performed in the future.

Among the three human glioma cell lines tested, MEK inhibitors increased PpIX accumulation in SNB75 (Figure 5) and U343 (Figure 7) but not in SF539 (Figure 6). This result was not surprising because we previously found that approximately 30% of human cancer cells do not promote PpIX accumulation when treated with a MEK inhibitor (Yoshioka et al., 2018). There are a few possible mechanisms for the different responses among the glioma cell lines. First, we reported that MEK inhibition promotes PpIX accumulation by reducing ABCB1 expression and FECH function (Yoshioka et al., 2018; Chelakkot et al., 2020). If a cancer cell line has aberrant activation of downstream elements of MEK, which regulates ABCB1 and FECH, MEK inhibition

will not increase PpIX accumulation. RSKs are considered to be responsible downstream elements of MEK regulating PpIX accumulation (Chelakkot et al., 2020). If RSKs are activated by another oncogenic pathway, PpIX accumulation could occur independently of the MEK pathway. Second, SF539 may not have a high activity level of the MEK pathway. Oncogenic cell lines without highly activated members of the RAS/MEK signaling pathway are unlikely to show sensitivity to MEK inhibitors. McCubrey et al. (2007) investigated prostate cancer cell lines with low MEK activity levels and reported no enhancement in PpIX fluorescence when treated with U0126 MEK inhibitor. If this is the case with SF539, MEK inhibition will not change accumulation levels of PpIX. However, to the best of my knowledge, no study looked at the activation level of different RAS and its effector pathways in SF539 cell line. To address this, we will need to compare phosphorylation levels of ERKs in SF539 to those in SNB75 or U343 by western blot analysis. Lastly, the potency of MEK inhibitors in upregulating PpIX may be limited unless the RAS/MEK pathway is directly responsible for the proliferation of the particular cancer type (McCubrey et al., 2010). One pathway that is often aberrantly hyperactivated in various types of cancer, including colorectal, breast, and GBM, is the PI3K pathway. A study by Wee et al. (2009) reported a loss of sensitivity to MEK inhibitors in multiple cancer cell lines that harbor an activating mutation in the PI3K pathway. Therefore, the resistance of SF539 cell line to MEK inhibitor-mediated PpIX upregulation suggests either a hyper-activated PI3K pathway instead of RAS/MEK contributing to its tumorigenesis or co-activation of both PI3K and RAS/MEK pathway resulting in masking of the MEK inhibition effect. To determine if SF539 cell line is resistant to the action of MEK inhibitors, we can perform a western blot analysis of phosphorylated ERK in the future.

4.2 *In vivo* Experimental Models

We faced several challenges when developing the *in vivo* brain tumor model. One of them was quenching of PpIX fluorescence due to exposure to light, as previously reported (Belykh et al., 2018). The exposure to light occurred at different sample preparation steps, such as mice brain tissue sectioning and coverslipping. Therefore, the preparation of brain samples and sections was conducted in a dark environment. Furthermore, we observed the fluorescence quenching of PpIX while taking images under the microscope. Another challenge we faced was the loss of PpIX fluorescence due to formalin fixation of the brain samples. Although I tried different durations of the fixation and fixative agents, we could not find optimal ways to fix the brain samples. Instead, we decided to use flash freezing of the brain samples in the OCT compound and section them using a cryotome, which is currently the best way to detect PpIX fluorescence in brain sections with tumors. With this method, we detected PpIX fluorescence of tumors in the brain sections (Fig 11B). Lastly, when brain sections were imaged again after 3-4 weeks, the samples were found to have lost PpIX fluorescence almost entirely. This observation led us to believe that PpIX molecules in tissues spontaneously decay when stored for an extended period. Therefore, the brain sections are not suitable for long term storage, and we suggest imaging the brain samples with PpIX molecules immediately after preparation.

For the PDD of brain tumors, it is essential for both 5-ALA and the MEK inhibitors to cross the blood brain barrier (BBB) to reach the tumors. The BBB is responsible for the selective uptake of various molecules from the peripheral bloodstream to the brain. It is comprised of a monolayer of endothelial cells, which are connected to each other by tight junctions, forming a physical barrier that protects the brain. Therefore, transport of molecules across the BBB happens mostly through paracellular transport or transcytosis, which is limited. This is the case for 5-ALA

as 5-ALA transport through the BBB is limited in healthy brains (Stepp & Stummer, 2018; Ennis et al., 2003). Similarly, other pre-clinical studies have demonstrated the limited ability of MEK inhibitors to penetrate the BBB, including Trametinib, Selumetinib, Binimetinib, and Cobimetinib (Gampa et al., 2018, Vaidhyanathan et al., 2014). An impaired brain penetration can limit the therapeutic efficacy of the MEK inhibitors against intracranial tumors. There are MEK inhibitors such as SL327 and E6201, which can penetrate the BBB (Zhao et al., 2012; Gampa et al., 2018). Unfortunately, these MEK inhibitors have not been tested in clinical trials for their safety and efficacy. However, the leakiness of the BBB under disease conditions has been reported (Sarkaria et al., 2018; Arvanitis et al., 2020; Stewart, 1994; Gampa et al., 2016). Especially in the case of brain tumors, the neo-vascularization caused during tumor development generates new and leaky blood vessels, which may allow the penetration of 5-ALA and other small molecules, such as MEK inhibitors, into the brain (Stepp & Stummer, 2018). However, other regions of such tumors, especially tumor edge and metastases, may have a relatively intact BBB (Gampa et al., 2018). Therefore, to improve the efficacy of 5-ALA-PDD, it is essential to identify other new ways to increase the penetration of 5-ALA and MEK inhibitors across the BBB. The polymeric nanocarriers could be one strategy for future study (Bikhezari et al., 2020).

4.3 Microscopic evaluation of PpIX fluorescence in brain tumors

In the *in vivo* experiments, we used mouse 4T1 breast cancer cells expressing GFP as a reference for tumor locations. As shown in Figure 11, we confirmed the co-localization of PpIX fluorescence and GFP in the brain sections using an epifluorescence microscope, suggesting that GFP is valuable as a reference for tumor locations. However, we found that GFP was much more resistant to fluorescence quenching than PpIX fluorescence.

We also used the 2-Photon microscopy analysis to evaluate PpIX fluorescence in brain tumors. We believe that the 2-Photon microscopy analysis is more suitable for future studies. This is because the photobleaching of PpIX fluorescence is less in the 2-Photon microscopy analysis than with epifluorescence microscope. Unlike epifluorescence microscopy, where the whole tissue section is exposed to light, the excitation of the fluorophore is achieved only at the optical section during 2-Photon microscopy. Therefore, photobleaching and photodamage to the regions above and below the focal plane are minimized. During the 2-Photon microscopy analysis, brain slices are kept alive, and tumor cells are capable of synthesizing PpIX, which would cause less technical variation caused by the photobleaching than the histological analysis. Furthermore, the 2-Photon microscopy analysis can generate 3-D images of the brain tumors, which give us a better evaluation of PpIX fluorescence at the tumor ends and in satellite tumors.

For 2-photon imaging analysis, we used brain slices from tumor-bearing mice injected with 5-ALA and with or without the MEK inhibitor Selumetinib (Figure 12). Alternatively, we could also treat the brain slice with the tumor with the MEK inhibitor *ex vivo* during 2-Photon microscopy analysis. This would allow us to compare PpIX fluorescence before and after treatment of the MEK inhibitor on the same brain slice.

In our study, we visualized PpIX fluorescence in both thin brain sections (20 μm) using traditional epifluorescence microscopy and thick brain sections (350 μm) using 2-Photon microscopy. 2-Photon microscopy is more suitable for imaging thick brain sections as there is a heightened possibility for photodamage of visible fluorescent probes, such as PpIX, in thin brain sections imaged using 2-Photon microscopy (Benninger & Piston, 2013).

Due to the heterogeneous tumor growth, glioma cell diversity, and differences in metabolism among glioma cells, 5-ALA mediated visual PpIX fluorescence in gliomas is typically

patchy with areas of high and low fluorescence intensity (Belykh et al., 2018). Tumor areas with strong PpIX fluorescence are associated with a solid tumor, while areas with low or vague fluorescence feature tumor infiltrating into normal tissue. This low intensity tumor fluorescence is often hard to visualize *in situ*, given that the signal amplitude from these tissues is an order of magnitude lower than that from a solid tumor (Stummer et al., 2000). This sub-optimal tumor fluorescence often results in a lack of clear visualization of tumor ends, leading to a problem where 5-ALA treatment alone may miss certain areas with tumor tissue during FGS and result in cancer regrowth. The preliminary results from 2-Photon microscopy of brain tumors show that Selumetinib treatment reserves the potential to overcome the suboptimal and non-homogenous PpIX distribution across tumor tissues. A substantial increase in PpIX fluorescence was observed in brain tumors treated with Selumetinib and 5-ALA compared to those treated only with 5-ALA. Additionally, the PpIX fluorescence with Selumetinib treatment was more robust and evenly distributed throughout the tumor mass, with tumor ends clearly visible. If this observation is further confirmed in the future, our research could offer a solution to the shortcomings of 5-ALA PDD/FGS in clinical settings.

The goal of my MSc research was to establish an experimental system to evaluate cancer specific PpIX fluorescence in animal models of brain tumors. I was able to collect only one brain tumor sample to evaluate the efficacy of MEK inhibitor treatment on PpIX fluorescence *in vivo*, which is not sufficient to conduct statistical analysis. Nevertheless, we have obtained preliminary findings using 2-photon microscopy indicating that treatment of a MEK inhibitor may improve the efficacy of 5-ALA FGS of brain tumors (Figure 12). However, we did not detect any obvious satellite tumors in the brain section. This may be because the 4T1 allograft model used in this study does not form satellite tumors in the brain. In the future, systemic injection of 4T1 to develop

animal models of breast cancer brain metastasis can be explored (Kim et al., 2018). It is also possible that the 2-Photon microscopy analysis is not sensitive enough to detect small tumors in the brain. Additionally, we may need to optimize the dosage of 5-ALA and MEK inhibitors or test other MEK inhibitors that were evaluated *in vitro* in our study. This remains to be clarified in Dr. Hirasawa's lab in the future.

4.5 Feasibility of MEK Inhibitors for Use in FGS Applications

In addition to improving the sensitivity of FGS, combination therapy of 5-ALA plus MEK inhibitor may offer a host of other advantages: 1) Given the antitumor properties of MEK inhibitors, they could work additively or synergistically with other anticancer treatments prescribed to the patient. For example, the upregulation of PpIX in cancer cells by MEK inhibition can promote cancer cell death induced by 5-ALA-PDT. 2) The use of a MEK inhibitor can potentially reduce the dosage of 5-ALA in patients, therefore reducing the side effects of 5-ALA such as hypotension, gastrointestinal, liver function, and hematological disorders experienced by patients (Kemmner et al., 2008; Teixidor et al., 2016; Chung & Eljamel, 2013). Therefore, we believe that using MEK inhibitors to improve 5-ALA FGS efficacy is realistic and could directly impact its applications in clinical settings.

4.6 Summary

Altogether, *in vitro* screening demonstrated Selumetinib and Trametinib to be the best MEK inhibitors for promoting PpIX accumulation in cancer cell lines. Although we evaluated the efficacy of Selumetinib *in vivo*, the potential of Trametinib in upregulating PpIX will be evaluated

in future studies. Our screening also revealed that 2 out of 3 glioma cell lines to be sensitive to the effect of MEK inhibitors to upregulate PpIX. In contrast, the other glioma cell line, SF539, was completely non-responsive. Therefore, it is crucial to investigate the cellular mechanisms that render certain cancer cell lines resistant to PpIX accumulation induced by MEK inhibition in the future. The commonly reported shortcomings of 5-ALA PDD/FGS were addressed with the application of Selumetinib during 2-Photon microscopy. Selumetinib treatment enhanced PpIX fluorescence in brain tumors and enhanced tumor end visualization. The preliminary findings from the *in vivo* studies warrant further animal and pre-clinical studies in the future. Both 5-ALA and several MEK inhibitors are already approved for clinical use, suggesting their safety. Therefore, a 5-ALA and MEK inhibitor combination treatment to enhance PpIX accumulation for FGS applications is a realistic approach and could directly impact patient outcomes in clinical settings.

Bibliography

Adjei, A.A., LoRusso, P., Ribas, A., Sosman, J.A., Pavlick, A., Dy, G.K., Zhou, X., Gangolli, E., Kneissl, M., Faucette, S., & Neuwirth, R. (2017). A phase I dose-escalation study of TAK-733, an investigational oral MEK inhibitor, in patients with advanced solid tumors. *Investigational New Drugs*, 35(1), 47-58. DOI: [10.1007/s10637-016-0391-2](https://doi.org/10.1007/s10637-016-0391-2)

Allison, R. R. (2015). Fluorescence guided resection (FGR): A primer for oncology. *Photodiagnosis and Photodynamic Therapy*, 13, 73-80. DOI: [10.1016/j.pdpdt.2015.11.008](https://doi.org/10.1016/j.pdpdt.2015.11.008)

Altunay, S. (2017). Role of Pathologist in Driver of Treatment of CNS Tumors. In *New Approaches to the Management of Primary and Secondary CNS Tumors*. IntechOpen. DOI:[10.5772/65911](https://doi.org/10.5772/65911)

American Cancer Society. (2020). *Chemotherapy side effects*. Retrieved July 2021, from [cancer.org/treatment/treatments-and-side-effects/treatment-types/chemotherapy/chemotherapy-side-effects.html](https://www.cancer.org/treatment/treatments-and-side-effects/treatment-types/chemotherapy/chemotherapy-side-effects.html)

American Cancer Society. Cancer Facts & Figures 2019. Atlanta: American Cancer Society; 2019.

American Cancer Society. Global Cancer Facts & Figures 4th Edition. Atlanta: American Cancer Society; 2018.

Arvanitis, C. D., Ferraro, G. B., & Jain, R. K. (2020). The blood–brain barrier and blood–tumor barrier in brain tumours and metastases. *Nature Reviews Cancer*, 20(1), 26-41. DOI: [10.1038/s41568-019-0205-x](https://doi.org/10.1038/s41568-019-0205-x)

Barnes, J. R., Mukherjee, B., Rogers, B. C., Nafar, F., Gosse, M., & Parsons, M. P. (2020). The relationship between glutamate dynamics and activity-dependent synaptic plasticity. *Journal of Neuroscience*, 40(14), 2793-2807. DOI: [10.1523/JNEUROSCI.1655-19.2020](https://doi.org/10.1523/JNEUROSCI.1655-19.2020)

Bartholomeusz, C., Oishi, T., Saso, H., Akar, U., Liu, P., Kondo, K., Kazansky, A., Krishnamurthy, S., Lee, J., Esteva, F.J., Kigawa, J. & Ueno, N. T. (2012). MEK1/2 Inhibitor Selumetinib (AZD6244) Inhibits Growth of Ovarian Clear Cell Carcinoma in a PEA-15–Dependent Manner in a Mouse Xenograft Model. *Molecular Cancer Therapeutics*, 11(2), 360-369. DOI: [10.1158/1535-7163.MCT-11-0400](https://doi.org/10.1158/1535-7163.MCT-11-0400)

Baskaran, R., Lee, J., & Yang, S. G. (2018). Clinical development of photodynamic agents and therapeutic applications. *Biomaterials Research*, 22(1), 1-8. DOI: [10.1186/s40824-018-0140-z](https://doi.org/10.1186/s40824-018-0140-z)

Becker, A. P., Sells, B. E., Haque, S. J., & Chakravarti, A. (2021). Tumor Heterogeneity in Glioblastomas: From Light Microscopy to Molecular Pathology. *Cancers*, 13(4), 761. DOI: [10.3390/cancers13040761](https://doi.org/10.3390/cancers13040761)

Belykh, E., Miller, E.J., Patel, A.A., Bozkurt, B., Yağmurlu, K., Robinson, T.R., Nakaji, P., Spetzler, R.F., Lawton, M.T., Nelson, L.Y. & Preul, M. C. (2018). Optical characterization of neurosurgical operating microscopes: quantitative fluorescence and assessment of PpIX photobleaching. *Scientific Reports*, 8(1), 1-14. DOI: [10.1038/s41598-018-30247-6](https://doi.org/10.1038/s41598-018-30247-6)

Benninger, R. K., & Piston, D. W. (2013). Two-photon excitation microscopy for the study of living cells and tissues. *Current Protocols in Cell Biology*, 59(1), 4-11. DOI: [10.1002/0471143030.cb0411s59](https://doi.org/10.1002/0471143030.cb0411s59)

Bikhezar, F., de Kruijff, R.M., van der Meer, A.J., Villa, G.T., van der Pol, S.M., Aragon, G.B., Garcia, A.G., Narayan, R.S., de Vries, H.E., Slotman, B.J., & Sminia, P. (2020). Preclinical evaluation of binimetinib (MEK162) delivered via polymeric nanocarriers in combination with radiation and temozolomide in glioma. *Journal of Neuro-Oncology*, 146(2), 239-246. DOI: [10.1007/s11060-019-03365-y](https://doi.org/10.1007/s11060-019-03365-y)

Canadian Cancer Society's Advisory Committee on Cancer Statistics. Canadian Cancer Statistics 2017. Toronto, ON: Canadian Cancer Society; 2017. Available at: cancer.ca/Canadian-CancerStatistics-2017-EN.pdf (accessed November 2020). June 2017 ISSN 0835-2976

Canadian Cancer Statistics Advisory Committee. Canadian Cancer Statistics 2019. Toronto, ON: Canadian Cancer Society; 2019. Available at: cancer.ca/Canadian-Cancer-Statistics-2019-EN (accessed November 2020). September 2019 ISSN 0835-2976

Chambard, J. C., Lefloch, R., Pouysségur, J., & Lenormand, P. (2007). ERK implication in cell cycle regulation. *Biochim. Biophys. Acta* 1773, 1299–1310. DOI: [10.1016/j.bbamcr.2006.11.010](https://doi.org/10.1016/j.bbamcr.2006.11.010)

Chelakkot, V.S., Liu, K., Yoshioka, E., Saha, S., Xu, D., Licursi, M., Dorward, A., & Hirasawa, K. (2020). MEK reduces cancer-specific PpIX accumulation through the RSK-ABCB1 and HIF-1 α -FECH axes. *Scientific Reports*, 10(1). DOI: [10.1038/s41598-020-79144-x](https://doi.org/10.1038/s41598-020-79144-x)

Chelakkot, V. S., Som, J., Yoshioka, E., Rice, C. P., Rutihinda, S. G., & Hirasawa, K. (2019). Systemic MEK inhibition enhances the efficacy of 5-aminolevulinic acid-photodynamic therapy. *British Journal of Cancer*, *121*(9), 758-767. DOI: [10.1038/s41416-019-0586-3](https://doi.org/10.1038/s41416-019-0586-3)

Cheng, Y., & Tian, H. (2017). Current development status of MEK inhibitors. *Molecules*, *22*(10), 1551. DOI: [10.3390/molecules22101551](https://doi.org/10.3390/molecules22101551)

Chung, I. W. H., & Eljamel, S. (2013). Risk factors for developing oral 5-aminolevulinic acid-induced side effects in patients undergoing fluorescence guided resection. *Photodiagnosis and Photodynamic Therapy*, *10*(4), 362-367. DOI: [10.1016/j.pdpdt.2013.03.007](https://doi.org/10.1016/j.pdpdt.2013.03.007)

Collaud, S., Juzeniene, A., Moan, J., & Lange, N. (2004). On the selectivity of 5-aminolevulinic acid-induced protoporphyrin IX formation. *Current Medicinal Chemistry-Anti-Cancer Agents*, *4*(3), 301-316. DOI: [10.2174/1568011043352984](https://doi.org/10.2174/1568011043352984)

Dhillon, A. S., Hagan, S., Rath, O., & Kolch, W. (2007). MAP kinase signalling pathways in cancer. *Oncogene*, *26*(22), 3279-3290. DOI: [10.1038/sj.onc.1210421](https://doi.org/10.1038/sj.onc.1210421)

Dong, Q., Dougan, D.R., Gong, X., Halkowycz, P., Jin, B., Kanouni, T., O'Connell, S.M., Scolah, N., Shi, L., Wallace, M.B., & Zhou, F. (2011). Discovery of TAK-733, a potent and selective MEK allosteric site inhibitor for the treatment of cancer. *Bioorganic & Medicinal Chemistry Letters*, *21*(5), 1315-1319. DOI: [10.1016/j.bmcl.2011.01.071](https://doi.org/10.1016/j.bmcl.2011.01.071)

Duncia, J.V., Santella III, J.B., Higley, C.A., Pitts, W.J., Wityak, J., Fietze, W.E., Rankin, F.W., Sun, J.H., Earl, R.A., Tabaka, A.C., & Teleha, C.A. (1998). MEK inhibitors: the chemistry and biological activity of U0126, its analogs, and cyclization products. *Bioorganic & Medicinal Chemistry Letters*, *8*(20), 2839-2844. DOI: [10.1016/s0960-894x\(98\)00522-8](https://doi.org/10.1016/s0960-894x(98)00522-8)

Dunst, S., & Tomancak, P. (2019). Imaging flies by fluorescence microscopy: principles, technologies, and applications. *Genetics*, *211*(1), 15-34. DOI: [10.1534/genetics.118.300227](https://doi.org/10.1534/genetics.118.300227)

Ennis, S.R., Novotny, A., Xiang, J., Shakui, P., Masada, T., Stummer, W., Smith, D.E., & Keep, R. F. (2003). Transport of 5-aminolevulinic acid between blood and brain. *Brain Research*, *959*(2), 226-234. DOI: [10.1016/s0006-8993\(02\)03749-6](https://doi.org/10.1016/s0006-8993(02)03749-6)

Falchook, G.S., Long, G.V., Kurzrock, R., Kim, K.B., Arkenau, T.H., Brown, M.P., Hamid, O., Infante, J.R., Millward, M., Pavlick, A.C., & Kefford, R. F. (2012). Dabrafenib in patients with

melanoma, untreated brain metastases, and other solid tumours: a phase 1 dose-escalation trial. *The Lancet*, 379(9829), 1893-1901. DOI: [10.1016/S0140-6736\(12\)60398-5](https://doi.org/10.1016/S0140-6736(12)60398-5)

Fischmann, T.O., Smith, C.K., Mayhood, T.W., Myers Jr, J.E., Reichert, P., Mannarino, A., Carr, D., Zhu, H., Wong, J., Yang, R.S., & Le, H.V. (2009). Crystal structures of MEK1 binary and ternary complexes with nucleotides and inhibitors. *Biochemistry*, 48(12), 2661-2674. DOI: [10.1021/bi801898e](https://doi.org/10.1021/bi801898e)

Flaherty, K.T., Robert, C., Hersey, P., Nathan, P., Garbe, C., Milhem, M., Demidov, L.V., Hassel, J.C., Rutkowski, P., Mohr, P., & Schadendorf, D. (2012). Improved survival with MEK inhibition in BRAF-mutated melanoma. *New England Journal of Medicine*, 367(2), 107-114. DOI: [10.1056/NEJMoa1203421](https://doi.org/10.1056/NEJMoa1203421)

Frankel, T.L., LaFemina, J., Bamboat, Z.M., D'Angelica, M.I., DeMatteo, R.P., Fong, Y., Kingham, T.P., Jarnagin, W.R. & Allen, P. J. (2013). Dysplasia at the surgical margin is associated with recurrence after resection of non-invasive intraductal papillary mucinous neoplasms. *HPB*, 15(10), 814-821. DOI: [10.1111/hpb.12137](https://doi.org/10.1111/hpb.12137)

Gampa, G., Kim, M., Cook-Rostie, N., Laramy, J.K., Sarkaria, J.N., Paradiso, L., DePalatis, L., & Elmquist, W. F. (2018). Brain distribution of a novel MEK inhibitor E6201: implications in the treatment of melanoma brain metastases. *Drug Metabolism and Disposition*, 46(5), 658-666. DOI: [10.1124/dmd.117.079194](https://doi.org/10.1124/dmd.117.079194)

Gampa, G., Vaidhyanathan, S., Wilken-Resman, B., Parrish, K. E., Markovic, S. N., Sarkaria, J. N., & Elmquist, W. F. (2016). Challenges in the delivery of therapies to melanoma brain metastases. *Current Pharmacology Reports*, 2(6), 309-325 DOI: [10.1007/s40495-016-0072-z](https://doi.org/10.1007/s40495-016-0072-z)

Georges, J.F., Valeri, A., Wang, H., Brooking, A., Kakareka, M., Cho, S.S., Al-Atrache, Z., Bamimore, M., Osman, H., Ifrach, J., & Yocom, S. (2019). Delta-aminolevulinic acid-mediated photodiagnoses in surgical oncology: a historical review of clinical trials. *Frontiers in Surgery*, 6, 45. DOI: [10.3389/fsurg.2019.00045](https://doi.org/10.3389/fsurg.2019.00045)

Gioux, S., Choi, H. S., & Frangioni, J. V. (2010). Image-guided surgery using invisible near-infrared light: fundamentals of clinical translation. *Molecular Imaging*, 9(5), 7290-2010 PMID: [PMC3105445](https://pubmed.ncbi.nlm.nih.gov/3105445/)

Goodenberger, M. L., & Jenkins, R. B. (2012). Genetics of adult glioma. *Cancer Genetics*, 205(12), 613-621. DOI: [10.1016/j.cancergen.2012.10.009](https://doi.org/10.1016/j.cancergen.2012.10.009)

Goryaynov, S.A., Widhalm, G., Goldberg, M.F., Chelushkin, D., Spallone, A., Chernyshov, K.A., Ryzhova, M., Pavlova, G., Revischin, A., Shishkina, L., & Potapov, A. (2019). The role of 5-ALA in low-grade gliomas and the influence of antiepileptic drugs on intraoperative fluorescence. *Frontiers in Oncology*, 9, 423. DOI: [10.3389/fonc.2019.00423](https://doi.org/10.3389/fonc.2019.00423)

Grimaldi, A. M., Simeone, E., Festino, L., Vanella, V., Strudel, M., & Ascierto, P. A. (2017). MEK inhibitors in the treatment of metastatic melanoma and solid tumors. *American Journal of Clinical Dermatology*, 18(6), 745-754. DOI: [10.1007/s40257-017-0292-y](https://doi.org/10.1007/s40257-017-0292-y)

Guyotat, J., Pallud, J., Armoiry, X., Pavlov, V., & Metellus, P. (2016). 5-aminolevulinic acid–protoporphyrin IX fluorescence-guided surgery of high-grade gliomas: a systematic review. *In Advances and Technical Standards in Neurosurgery* (pp. 61-90). Springer, Cham. DOI: [10.1007/978-3-319-21359-0_3](https://doi.org/10.1007/978-3-319-21359-0_3)

Gysin, S., Lee, S. H., Dean, N. M., & McMahon, M. (2005). Pharmacologic inhibition of RAF→MEK→ERK signaling elicits pancreatic cancer cell cycle arrest through induced expression of p27Kip1. *Cancer Research*, 65(11), 4870-4880. DOI: [10.1158/0008-5472.CAN-04-2848](https://doi.org/10.1158/0008-5472.CAN-04-2848)

Hadjipanayis, C. G., & Stummer, W. (2019). 5-ALA and FDA approval for glioma surgery. *Journal of Neuro-Oncology*, 141(3), 479-486. DOI: [10.1007/s11060-019-03098-y](https://doi.org/10.1007/s11060-019-03098-y)

Hanif, F., Muzaffar, K., Perveen, K., Malhi, S. M., & Simjee, S. U. (2017). Glioblastoma multiforme: a review of its epidemiology and pathogenesis through clinical presentation and treatment. *Asian Pacific Journal of Cancer Prevention: APJCP*, 18(1), 3. DOI: [10.22034/APJCP.2017.18.1.3](https://doi.org/10.22034/APJCP.2017.18.1.3)

Hawkins, T. A., Cavodeassi, F., Erdélyi, F., Szabó, G., & Lele, Z. (2008). The small molecule Mek1/2 inhibitor U0126 disrupts the chordamesoderm to notochord transition in zebrafish. *BMC Developmental Biology*, 8(1), 1-18. DOI: [10.1186/1471-213X-8-42](https://doi.org/10.1186/1471-213X-8-42)

Hendricks, B. K., Sanai, N., & Stummer, W. (2018). Fluorescence-guided surgery with aminolevulinic acid for low-grade gliomas. *Journal of Neuro-Oncology*, 141(1), 13-18. DOI: [10.1007/s11060-018-03026-6](https://doi.org/10.1007/s11060-018-03026-6)

Huang, Z. (2005). A review of progress in clinical photodynamic therapy. *Technology in Cancer Research & Treatment*, 4(3), 283-293. DOI: [10.1177/153303460500400308](https://doi.org/10.1177/153303460500400308)

Inoue, K. (2017). 5-Aminolevulinic acid-mediated photodynamic therapy for bladder cancer. *International Journal of Urology*, 24(2), 97-101. DOI: [10.1111/iju.13291](https://doi.org/10.1111/iju.13291)

Ishizuka, M., Abe, F., Sano, Y., Takahashi, K., Inoue, K., Nakajima, M., Kohda, T., Komatsu, N., Ogura, S.I. & Tanaka, T. (2011). Novel development of 5-aminolevulinic acid (ALA) in cancer diagnoses and therapy. *International Immunopharmacology*, 11(3), 358-365. DOI: [10.1016/j.intimp.2010.11.029](https://doi.org/10.1016/j.intimp.2010.11.029)

Jaber, M., Wölfer, J., Ewelt, C., Holling, M., Hasselblatt, M., Niederstadt, T., Zoubi, T., Weckesser, M., & Stummer, W. (2016). The value of 5-aminolevulinic acid in low-grade gliomas and high-grade gliomas lacking glioblastoma imaging features: an analysis based on fluorescence, magnetic resonance imaging, 18F-fluoroethyl tyrosine positron emission tomography, and tumor molecular factors. *Neurosurgery*, 78(3), 401-411. DOI: [10.1227/NEU.0000000000001020](https://doi.org/10.1227/NEU.0000000000001020)

Jolesz, F. A. (Ed.). (2014). *Intraoperative imaging and image-guided therapy*. Springer Science & Business Media.

Kaneko, S., & Kaneko, S. (2016). Fluorescence-guided resection of malignant glioma with 5-ALA. *International Journal of Biomedical Imaging*, 2016. DOI: [10.1155/2016/6135293](https://doi.org/10.1155/2016/6135293)

Kemmner, W., Wan, K., Rüttinger, S., Ebert, B., Macdonald, R., Klamm, U., & Moesta, K. T. (2008). Silencing of human ferrochelatase causes abundant protoporphyrin-IX accumulation in colon cancer. *The FASEB Journal*, 22(2), 500-509. DOI: [10.1096/fj.07-8888com](https://doi.org/10.1096/fj.07-8888com)

Khong, A., Cleaver, A.L., Alatas, M.F., Wylie, B.C., Connor, T., Fisher, S.A., Broomfield, S., Lesterhuis, W.J., Currie, A.J., Lake, R.A., & Robinson, B. W. (2014). The efficacy of tumor debulking surgery is improved by adjuvant immunotherapy using imiquimod and anti-CD40. *BMC Cancer*, 14(1), 1-9. DOI: [10.1186/1471-2407-14-969](https://doi.org/10.1186/1471-2407-14-969)

Kim, S.H., Redvers, R.P., Chi, L.H., Ling, X., Lucke, A.J., Reid, R.C., Fairlie, D.P., Martin, A.C.B.M., Anderson, R.L., Denoyer, D., & Pouliot, N. (2018). Identification of brain metastasis genes and therapeutic evaluation of histone deacetylase inhibitors in a clinically relevant model of breast cancer brain metastasis. *Disease Models & Mechanisms*, 11(7), DMM034850. DOI: [10.1242/dmm.034850](https://doi.org/10.1242/dmm.034850)

Kishi, Y., Okudaira, S., Tanaka, M., Hama, K., Shida, D., Kitayama, J., Yamori, T., Aoki, J., Fujimaki, T., & Arai, H. (2006). Autotaxin is overexpressed in glioblastoma multiforme and

contributes to cell motility of glioblastoma by converting lysophosphatidylcholine to lysophosphatidic acid. *Journal of Biological Chemistry*, 281(25), 17492-17500. DOI: [10.1074/jbc.M601803200](https://doi.org/10.1074/jbc.M601803200)

Kitajima, Y., Ishii, T., Kohda, T., Ishizuka, M., Yamazaki, K., Nishimura, Y., Tanaka, T., Dan, S., & Nakajima, M. (2019). Mechanistic study of PpIX accumulation using the JFCR39 cell panel revealed a role for dynamin 2-mediated exocytosis. *Scientific Reports*, 9(1), 1-11. DOI: [10.1038/s41598-019-44981-y](https://doi.org/10.1038/s41598-019-44981-y)

Knight, T., & Irving, J. A. E. (2014). Ras/Raf/MEK/ERK Pathway activation in childhood acute lymphoblastic leukemia and its therapeutic targeting. *Front. Oncol.* 4:160. DOI: [10.3389/fonc.2014.00160](https://doi.org/10.3389/fonc.2014.00160)

Kobuchi, H., Moriya, K., Ogino, T., Fujita, H., Inoue, K., Shuin, T., Yasuda, T., Utsumi, K., & Utsumi, T. (2012). Mitochondrial localization of ABC transporter ABCG2 and its function in 5-aminolevulinic acid-mediated protoporphyrin IX accumulation. *PloS One*, 7(11), DOI: [10.1371/journal.pone.0050082](https://doi.org/10.1371/journal.pone.0050082)

Lee, S., Rauch, J., & Kolch, W. (2020). Targeting MAPK signaling in cancer: mechanisms of drug resistance and sensitivity. *International Journal of Molecular Sciences*, 21(3), 1102 DOI: [10.3390/ijms21031102](https://doi.org/10.3390/ijms21031102)

Liang, H., Liu, T., Chen, F., Liu, Z., & Liu, S. (2011). A full-length 3D structure for MAPK/ERK kinase 2 (MEK2). *Science China Life Sciences*, 54(4), 336-341. DOI: [10.1007/s11427-011-4156-z](https://doi.org/10.1007/s11427-011-4156-z)

Liu, F., Yang, X., Geng, M., & Huang, M. (2018). Targeting ERK, an Achilles' Heel of the MAPK pathway, in cancer therapy. *Acta Pharmaceutica Sinica B*, 8(4), 552-562. DOI: [10.1016/j.apsb.2018.01.008](https://doi.org/10.1016/j.apsb.2018.01.008)

Liu, R., Xu, Y., Xu, K., & Dai, Z. (2021). Current trends and key considerations in the clinical translation of targeted fluorescent probes for intraoperative navigation. *Aggregate*. DOI: <https://doi.org/10.1002/agt2.23>

Louis, D.N., Ohgaki, H., Wiestler, O.D., Cavenee, W.K., Burger, P.C., Jouvett, A., Scheithauer, B.W. & Kleihues, P. (2007). The 2007 WHO classification of tumours of the central nervous system. *Acta Neuropathologica*, 114(2), 97-109. DOI: [10.1007/s00401-007-0243-4](https://doi.org/10.1007/s00401-007-0243-4)

Luke, J. J., Ott, P. A., & Shapiro, G. I. (2014). The biology and clinical development of MEK inhibitors for cancer. *Drugs*, 74(18), 2111-2128. DOI: [10.1007/s40265-014-0315-4](https://doi.org/10.1007/s40265-014-0315-4)

Mabray, M. C., Barajas, R. F., & Cha, S. (2015). Modern brain tumor imaging. *Brain Tumor Research and Treatment*, 3(1), 8-23. DOI: [10.14791/btrt.2015.3.1.8](https://doi.org/10.14791/btrt.2015.3.1.8)

Maletínská, L., Blakely, E. A., Bjornstad, K. A., Deen, D. F., Knoff, L. J., & Forte, T. M. (2000). Human glioblastoma cell lines: levels of low-density lipoprotein receptor and low-density lipoprotein receptor-related protein. *Cancer Research*, 60(8), 2300-2303.

Marampon, F., Bossi, G., Ciccarelli, C., Di Rocco, A., Sacchi, A., Pestell, R. G., & Zani, B. M. (2009). MEK/ERK inhibitor U0126 affects in vitro and in vivo growth of embryonal rhabdomyosarcoma. *Molecular Cancer Therapeutics*, 8(3), 543-551. DOI: [10.1158/1535-7163.MCT-08-0570](https://doi.org/10.1158/1535-7163.MCT-08-0570)

Marta, G. N., Correa, S. F. M., & Teixeira, M. J. (2011). Meningioma: review of the literature with emphasis on the approach to radiotherapy. *Expert Review of Anticancer Therapy*, 11(11), 1749-1758. DOI: [10.1586/era.11.162](https://doi.org/10.1586/era.11.162)

Matsui, A., Tanaka, E., Choi, H.S., Winer, J.H., Kianzad, V., Gioux, S., Laurence, R.G. & Frangioni, J. V. (2010). Real-time intra-operative near-infrared fluorescence identification of the extrahepatic bile ducts using clinically available contrast agents. *Surgery*, 148(1), 87-95. DOI: [10.1016/j.surg.2009.12.004](https://doi.org/10.1016/j.surg.2009.12.004)

McCubrey, J.A., Steelman, L.S., Abrams, S.L., Chappell, W.H., Russo, S., Ove, R., Milella, M., Tafuri, A., Lunghi, P., Bonati, A., & Stivala, F. (2010). Emerging MEK inhibitors. *Expert Opinion on Emerging Drugs*, 15(2), 203-223., 2010. DOI: [10.1517/14728210903282760](https://doi.org/10.1517/14728210903282760)

McCubrey, J.A., Steelman, L.S., Chappell, W.H., Abrams, S.L., Wong, E.W., Chang, F., Lehmann, B., Terrian, D.M., Milella, M., Tafuri, A., & Franklin, R. A. (2007). Roles of the Raf/MEK/ERK pathway in cell growth, malignant transformation and drug resistance. *Biochimica et Biophysica Acta (BBA)-Molecular Cell Research*, 1773(8), 1263-1284. DOI: [10.1016/j.bbamcr.2006.10.001](https://doi.org/10.1016/j.bbamcr.2006.10.001)

Mendez, J. S., & DeAngelis, L. M. (2018). Metastatic complications of cancer involving the central and peripheral nervous systems. *Neurologic Clinics*, 36(3), 579-598. DOI: [10.1016/j.ncl.2018.04.011](https://doi.org/10.1016/j.ncl.2018.04.011)

Mesfin, F. B., & Al-Dhahir, M. A. (2020). *Cancer, Brain Gliomas. Treasure Island (FL): Statpearls Publishing.*

Metildi, C.A., Kaushal, S., Hardamon, C.R., Snyder, C.S., Pu, M., Messer, K.S., Talamini, M.A., Hoffman, R.M. & Bouvet, M. (2012). Fluorescence-guided surgery allows for more complete resection of pancreatic cancer, resulting in longer disease-free survival compared with standard surgery in orthotopic mouse models. *Journal of the American College of Surgeons*, 215(1), 126-135. DOI: [10.1016/j.jamcollsurg.2012.02.021](https://doi.org/10.1016/j.jamcollsurg.2012.02.021)

Millon, S. R., Ostrander, J. H., Yazdanfar, S., Brown, J. Q., Bender, J. E., Rajeha, A., & Ramanujam, N. (2010). Preferential accumulation of 5-aminolevulinic acid-induced protoporphyrin IX in breast cancer: a comprehensive study on six breast cell lines with varying phenotypes. *Journal of Biomedical Optics*, 15(1), 018002.) DOI: [10.1117/1.3302811](https://doi.org/10.1117/1.3302811)

Moiyadi, A., Syed, P., & Srivastava, S. (2014). Fluorescence-guided surgery of malignant gliomas based on 5-aminolevulinic acid: paradigm shifts but not a panacea. *Nature Reviews Cancer*, 14(2), 146-146. DOI: [10.1038/nrc3566-c1](https://doi.org/10.1038/nrc3566-c1)

Mondal, S. B., Gao, S., Zhu, N., Liang, R., Gruev, V., & Achilefu, S. (2014). Real-time fluorescence image-guided oncologic surgery. *In Advances in Cancer Research* (Vol. 124, pp. 171-211). Academic Press. DOI: [10.1016/B978-0-12-411638-2.00005-7](https://doi.org/10.1016/B978-0-12-411638-2.00005-7)

Moon, D. O., Park, C., Heo, M. S., Park, Y. M., Choi, Y. H., & Kim, G. Y. (2007). PD98059 triggers G1 arrest and apoptosis in human leukemic U937 cells through downregulation of Akt signal pathway. *International Immunopharmacology*, 7(1), 36-45. DOI: [10.1016/B978-0-12-411638-2.00005-7](https://doi.org/10.1016/B978-0-12-411638-2.00005-7)

Nagaya, T., Nakamura, Y. A., Choyke, P. L., & Kobayashi, H. (2017). Fluorescence-guided surgery. *Frontiers in Oncology*, 7, 314. DOI: [10.3389/fonc.2017.00314](https://doi.org/10.3389/fonc.2017.00314)

National Cancer Institute. (2019, January 8). *Radiation Therapy for Cancer*. Retrieved July 2021, from <https://www.cancer.gov/about-cancer/treatment/types/radiation-therapy#HRTWAC>

National Health Service. (2020, March 2). *Radiotherapy Side effects*. Nhs.Uk. Retrieved July 2021, from <https://www.nhs.uk/conditions/radiotherapy/side-effects>

Neuzillet, C., Tijeras-Raballand, A., de Mestier, L., Cros, J., Faivre, S., & Raymond, E. (2014).

MEK in cancer and cancer therapy. *Pharmacology & Therapeutics*, 141(2), 160-171.
DOI: [10.1016/j.pharmthera.2013.10.001](https://doi.org/10.1016/j.pharmthera.2013.10.001)

Nguyen, Q. T., & Tsien, R. Y. (2013). Fluorescence-guided surgery with live molecular navigation—a new cutting edge. *Nature Reviews Cancer*, 13(9), 653-662. DOI: [10.1038/nrc3566](https://doi.org/10.1038/nrc3566)

O'Donnell, P.W., Griffin, A.M., Eward, W.C., Sternheim, A., Catton, C.N., Chung, P.W., O'Sullivan, B., Ferguson, P.C., & Wunder, J. S. (2014). The effect of the setting of a positive surgical margin in soft tissue sarcoma. *Cancer*, 120(18), 2866-2875. DOI: [10.1002/cncr.28793](https://doi.org/10.1002/cncr.28793)

Ohren, J.F., Chen, H., Pavlovsky, A., Whitehead, C., Zhang, E., Kuffa, P., Yan, C., McConnell, P., Spessard, C., Banotai, C., & Mueller, W. T. (2004). Structures of human MAP kinase kinase 1 (MEK1) and MEK2 describe novel noncompetitive kinase inhibition. *Nature Structural & Molecular Biology*, 11(12), 1192-1197. DOI: [10.1038/nsmb859](https://doi.org/10.1038/nsmb859)

Ostrom, Q.T., Bauchet, L., Davis, F.G., Deltour, I., Fisher, J.L., Langer, C.E., Pekmezci, M., Schwartzbaum, J.A., Turner, M.C., Walsh, K.M., & Barnholtz-Sloan, J. S. (2014). The epidemiology of glioma in adults: a “state of the science” review. *Neuro-Oncology*, 16(7), 896-913. DOI: [10.1093/neuonc/nou087](https://doi.org/10.1093/neuonc/nou087)

Patel A. Benign vs Malignant Tumors. *JAMA Oncol.* 2020;6(9):1488.
DOI:10.1001/jamaoncol.2020.2592

Pichlmeier, U., Bink, A., Schackert, G., & Stummer, W. (2008). Resection and survival in glioblastoma multiforme: an RTOG recursive partitioning analysis of ALA study patients. *Neuro-Oncology*, 10(6), 1025-1034. DOI: [10.1215/15228517-2008-052](https://doi.org/10.1215/15228517-2008-052)

Polikarpov, D.M., Campbell, D.H., McRobb, L.S., Wu, J., Lund, M.E., Lu, Y., Deyev, S.M., Davidson, A.S., Walsh, B.J., Zvyagin, A.V., & Gillatt, D. A. (2020). Near-Infrared Molecular Imaging of Glioblastoma by Miltuximab®-IRDye800CW as a Potential Tool for Fluorescence-Guided Surgery. *Cancers*, 12(4), 984. DOI: [10.3390/cancers12040984](https://doi.org/10.3390/cancers12040984)

Ponka, P. (1999). Cell biology of heme. *The American Journal of the Medical Sciences*, 318(4), 241-256. DOI: [10.1097/00000441-199910000-00004](https://doi.org/10.1097/00000441-199910000-00004)

Primeau, A.S. (2018, November 30). *Cancer Recurrence Statistics*. Cancer Therapy Advisor.

Retrieved July 13, 2020 from <https://www.cancertherapyadvisor.com/home/tools/factsheets/cancer-recurrence-statistics>

Pulaski, B. A., & Ostrand-Rosenberg, S. (2000). Mouse 4T1 breast tumor model. *Current Protocols in Immunology*, 39(1), 20-2. DOI: [10.1002/0471142735.im2002s39](https://doi.org/10.1002/0471142735.im2002s39)

Raguz, S., & Yagüe, E. (2008). Resistance to chemotherapy: new treatments and novel insights into an old problem. *British Journal of Cancer*, 99(3), 387-391. DOI: [10.1038/sj.bjc.6604510](https://doi.org/10.1038/sj.bjc.6604510)

Ramanujam, N. (2000). Fluorescence spectroscopy of neoplastic and non-neoplastic tissues. *Neoplasia*, 2(1-2), 89-117. DOI: [10.1038/sj.neo.7900077](https://doi.org/10.1038/sj.neo.7900077)

Roberts, D.W., Valdés, P.A., Harris, B.T., Hartov, A., Fan, X., Ji, S., Leblond, F., Tosteson, T.D., Wilson, B.C., & Paulsen, K. D. (2012). Glioblastoma multiforme treatment with clinical trials for surgical resection (aminolevulinic acid). *Neurosurgery Clinics of North America*, 23(3), 371. DOI: [10.1016/j.nec.2012.04.001](https://doi.org/10.1016/j.nec.2012.04.001)

Roberts, P. J., & Der, C. J. (2007). Targeting the Raf-MEK-ERK mitogen-activated protein kinase cascade for the treatment of cancer. *Oncogene*, 26(22), 3291-3310. DOI: [10.1038/sj.onc.1210422](https://doi.org/10.1038/sj.onc.1210422)

Rocks, O., Peyker, A., & Bastiaens, P. I. (2006). Spatio-temporal segregation of Ras signals: one ship, three anchors, many harbors. *Current Opinion in Cell Biology*, 18(4), 351-357. DOI: [10.1016/j.ceb.2006.06.007](https://doi.org/10.1016/j.ceb.2006.06.007)

Rutka, J.T., Giblin, J.R., Høifødt, H.K., Dougherty, D.V., Bell, C.W., McCulloch, J.R., Davis, R.L., Wilson, C.B., & Rosenblum, M. L. (1986). Establishment and characterization of a cell line from a human gliosarcoma. *Cancer Research*, 46(11), 5893-5902.

Ryu, S. H., Heo, S. H., Park, E. Y., Choi, K. C., Ryu, J. W., Lee, S. H., & Lee, S. W. (2017). Selumetinib inhibits melanoma metastasis to mouse liver via suppression of EMT-targeted genes. *Anticancer Research*, 37(2), 607-614. DOI: [10.21873/anticancer.11354](https://doi.org/10.21873/anticancer.11354)

Santarpia, L., Lippman, S. M., & El-Naggar, A. K. (2012). Targeting the MAPK–RAS–RAF signaling pathway in cancer therapy. *Expert Opinion on Therapeutic Targets*, 16(1), 103-119. DOI: [10.1517/14728222.2011.645805](https://doi.org/10.1517/14728222.2011.645805)

Sarkaria, J.N., Hu, L.S., Parney, I.F., Pafundi, D.H., Brinkmann, D.H., Laack, N.N., Giannini, C., Burns, T.C., Kizilbash, S.H., Laramy, J.K., & Elmquist, W. F. (2018). Is the blood–brain barrier really disrupted in all glioblastomas? A critical assessment of existing clinical data. *Neuro-Oncology*, *20*(2), 184-191. DOI: [10.1093/neuonc/nox175](https://doi.org/10.1093/neuonc/nox175)

Schroeder, K., & Gururangan, S. (2014). Molecular variants and mutations in medulloblastoma. *Pharmacogenomics and Personalized Medicine*, *7*, 43. DOI: [10.2147/PGPM.S38698](https://doi.org/10.2147/PGPM.S38698)

Schubbert, S., Shannon, K., & Bollag, G. (2007). Hyperactive Ras in developmental disorders and cancer. *Nature Reviews Cancer*, *7*(4), 295-308. DOI: [10.1038/nrc2109](https://doi.org/10.1038/nrc2109)

Selvasarayanan, K. D., Wiederspohn, N., Hadzalic, A., Strobel, H., Payer, C., Schuster, A., ... & Westhoff, M. A. (2020). The limitations of targeting MEK signalling in Glioblastoma therapy. *Scientific reports*, *10*(1), 1-14. DOI: [10.1038/s41598-020-64289-6](https://doi.org/10.1038/s41598-020-64289-6)

Sevick-Muraca, E. M., & Rasmussen, J. C. (2008). Molecular imaging with optics: primer and case for near-infrared fluorescence techniques in personalized medicine. *Journal of Biomedical Optics*, *13*(4), 041303. DOI: [10.1117/1.2953185](https://doi.org/10.1117/1.2953185)

Shaul, Y. D., & Seger, R. (2007). The MEK/ERK cascade: From signaling specificity to diverse functions. *Biochim. Biophys. Acta* *1773*, 1213–1226. doi: [10.1016/j.bbamcr.2006.10.00](https://doi.org/10.1016/j.bbamcr.2006.10.00). DOI: [10.1016/j.bbamcr.2006.10.005](https://doi.org/10.1016/j.bbamcr.2006.10.005)

Silva, S., Sethi, A., Prabhu, V., Anderson, D., & Melian, E. (2015). MNGO-19 RETROSPECTIVE REVIEW OF OVERALL SURVIVAL IN MENINGIOMA PATIENTS TREATED WITH RADIOTHERAPY OR COMBINED RADIOTHERAPY AND SURGERY. *Neuro-Oncology*, *17*(Suppl 5), v134. Doi: [10.1093/neuonc/nov220.18](https://doi.org/10.1093/neuonc/nov220.18)

Smalley, K. S. M., & Flaherty, K. T. (2009). Integrating BRAF/MEK inhibitors into combination therapy for melanoma. *British journal of cancer*, *100*(3), 431-435. Doi: [10.1038/sj.bjc.6604891](https://doi.org/10.1038/sj.bjc.6604891)

Soares-Silva, M., Diniz, F. F., Gomes, G. N., & Bahia, D. (2016). The mitogen-activated protein kinase (MAPK) pathway: role in immune evasion by trypanosomatids. *Frontiers in Microbiology*, *7*, 183. DOI: [10.3389/fmicb.2016.00183](https://doi.org/10.3389/fmicb.2016.00183)

Spain, L., Goode, E., McGovern, Y., Joshi, K., & Larkin, J. (2016). The combination of vemurafenib and cobimetinib in advanced melanoma. *Expert Opinion on Orphan Drugs*, 4(11), 1105-1111. <https://doi.org/10.1080/21678707.2016.1241707>

Stepp, H., & Stummer, W. (2018). 5-ALA in the management of malignant glioma. *Lasers in Surgery and Medicine*, 50(5), 399-419. DOI: [10.1002/lsm.22933](https://doi.org/10.1002/lsm.22933)

Stewart, B. W., & Wild, C. P. (2014). *IARC Publications*. Website - World Cancer Report 2014. <https://publications.iarc.fr/Non-Series-Publications/World-Cancer-Reports/World-Cancer-Report-2014>

Stewart, D. J. (1994). A critique of the role of the blood-brain barrier in the chemotherapy of human brain tumors. *Journal of Neuro-Oncology*, 20(2), 121-139. DOI: [10.1007/BF01052723](https://doi.org/10.1007/BF01052723)

Stummer, W., Novotny, A., Stepp, H., Goetz, C., Bise, K., & Reulen, H. J. (2000). Fluorescence-guided resection of glioblastoma multiforme utilizing 5-ALA-induced porphyrins: a prospective study in 52 consecutive patients. *Journal of Neurosurgery*, 93(6), 1003-1013. DOI: [10.3171/jns.2000.93.6.1003](https://doi.org/10.3171/jns.2000.93.6.1003)

Stummer, W., Pichlmeier, U., Meinel, T., Wiestler, O. D., Zanella, F., Reulen, H. J., & ALA-Glioma Study Group. (2006). Fluorescence-guided surgery with 5-aminolevulinic acid for resection of malignant glioma: a randomised controlled multicentre phase III trial. *The Lancet Oncology*, 7(5), 392-401. DOI: [10.1016/S1470-2045\(06\)70665-9](https://doi.org/10.1016/S1470-2045(06)70665-9)

Stummer, W., Stepp, H., Möller, G., Ehrhardt, A., Leonhard, M., & Reulen, H. J. (1998). Technical principles for protoporphyrin-IX-fluorescence guided microsurgical resection of malignant glioma tissue. *Acta Neurochirurgica*, 140(10), 995-1000. DOI: [10.1007/s007010050206](https://doi.org/10.1007/s007010050206)

Teixidor, P., Arráez, M. Á., Villalba, G., Garcia, R., Tardaguila, M., González, J. J., Rimbau, J., Vidal, X., & Montane, E. (2016). Safety and efficacy of 5-aminolevulinic acid for high grade glioma in usual clinical practice: a prospective cohort study. *PloS One*, 11(2), e0149244. DOI: [10.1371/journal.pone.0149244](https://doi.org/10.1371/journal.pone.0149244)

Tonn, J. C., & Stummer, W. (2008). Fluorescence-guided resection of malignant gliomas using 5-aminolevulinic acid: practical use, risks, and pitfalls. *Clin Neurosurg*, 55(3), 20-26.

Tsugu, A., Ishizaka, H., Mizokami, Y., Osada, T., Baba, T., Yoshiyama, M., Nishiyama, J., & Matsumae, M. (2011). Impact of the combination of 5-aminolevulinic acid–induced fluorescence with intraoperative magnetic resonance imaging–guided surgery for glioma. *World Neurosurgery*, 76(1-2), 120-127. DOI: [10.1016/j.wneu.2011.02.005](https://doi.org/10.1016/j.wneu.2011.02.005)

U.S. Food and Drug Administration. (2020, April 13). *FDA approves selumetinib for neurofibromatosis type 1 with symptomatic*. Retrieved June 21, 2021, from <https://www.fda.gov/drugs/resources-information-approved-drugs/fda-approves-selumetinib-neurofibromatosis-type-1-symptomatic-inoperable-plexiform-neurofibromas>

Vahrmeijer, A. L., Hutteman, M., Van Der Vorst, J. R., Van De Velde, C. J., & Frangioni, J. V. (2013). Image-guided cancer surgery using near-infrared fluorescence. *Nature Reviews Clinical Oncology*, 10(9), 507. DOI: [10.1038/nrclinonc.2013.123](https://doi.org/10.1038/nrclinonc.2013.123)

Vaidyanathan, S., Mittapalli, R. K., Sarkaria, J. N., & Elmquist, W. F. (2014). Factors influencing the CNS distribution of a novel MEK-1/2 inhibitor: implications for combination therapy for melanoma brain metastases. *Drug Metabolism and Disposition*, 42(8), 1292-1300. DOI: [10.1124/dmd.114.058339](https://doi.org/10.1124/dmd.114.058339)

Valdés, P.A., Kim, A., Brantsch, M., Niu, C., Moses, Z.B., Tosteson, T.D., Wilson, B.C., Paulsen, K.D., Roberts, D.W. & Harris, B. T. (2011). δ -aminolevulinic acid–induced protoporphyrin IX concentration correlates with histopathologic markers of malignancy in human gliomas: the need for quantitative fluorescence-guided resection to identify regions of increasing malignancy. *Neuro-Oncology*, 13(8), 846-856. DOI: [10.1093/neuonc/nor086](https://doi.org/10.1093/neuonc/nor086)

van Manen, L., Handgraaf, H. J., Diana, M., Dijkstra, J., Ishizawa, T., Vahrmeijer, A. L., & Mieog, J. S. D. (2018). A practical guide for the use of indocyanine green and methylene blue in fluorescence-guided abdominal surgery. *Journal of Surgical Oncology*, 118(2), 283-300. DOI: [10.1002/jso.25105](https://doi.org/10.1002/jso.25105)

Vanneman, M., & Dranoff, G. (2012). Combining immunotherapy and targeted therapies in cancer treatment. *Nature Reviews Cancer*, 12(4), 237-251. DOI: [10.1038/nrc3237](https://doi.org/10.1038/nrc3237)

Vicente, N. B., Zamboni, J. E. D., Adur, J. F., Paravani, E. V., & Casco, V. H. (2007, November). Photobleaching correction in fluorescence microscopy images. In *Journal of Physics: Conference Series* (Vol. 90, No. 1, p. 012068). IOP Publishing.

Wachowska, M., Muchowicz, A., Firczuk, M., Gabrysiak, M., Winiarska, M., Wańczyk, M., Bojarczuk, K. & Golab, J. (2011). Aminolevulinic acid (ALA) as a prodrug in photodynamic therapy of cancer. *Molecules*, 16(5), 4140-4164. Doi: [10.3390/molecules16054140](https://doi.org/10.3390/molecules16054140)

Wang, C., Chen, X., Wu, J., Liu, H., Ji, Z., Shi, H., Gao, C., Han, D., Wang, L., Liu, Y., & Zhao, S. (2013). Low-dose arsenic trioxide enhances 5-aminolevulinic acid-induced PpIX accumulation and efficacy of photodynamic therapy in human glioma. *Journal of Photochemistry and Photobiology B: Biology*, 127, 61-67. DOI: [10.1016/j.jphotobiol.2013.06.001](https://doi.org/10.1016/j.jphotobiol.2013.06.001)

Wang, D., Ma, D., Wong, M. L., & Wang, Y. X. J. (2015). Recent advances in surgical planning & navigation for tumor biopsy and resection. *Quantitative Imaging in Medicine and Surgery*, 5(5), 640. DOI: [10.3978/j.issn.2223-4292.2015.10.03](https://doi.org/10.3978/j.issn.2223-4292.2015.10.03)

Warnick, R., McPherson, C., & Gozal, Y. (2019, September). *Brain tumors: an introduction*. Mayfield. Retrieved July 12, 2020 from <https://mayfieldclinic.com/pe-braintumor.htm#:~:text=A%20brain%20tumor%20is%20an,tumor%20type%2C%20size%20and%20location>

Wee, S., Jagani, Z., Xiang, K.X., Loo, A., Dorsch, M., Yao, Y.M., Sellers, W.R., Lengauer, C., & Stegmeier, F. (2009). PI3K pathway activation mediates resistance to MEK inhibitors in KRAS mutant cancers. *Cancer Research*, 69(10), 4286-4293. DOI: [10.1158/0008-5472.CAN-08-4765](https://doi.org/10.1158/0008-5472.CAN-08-4765)

World Health Organization. (2018, September 12). *Cancer*. <https://www.who.int/news-room/fact-sheets/detail/cancer>

Yang, X., Palasuberniam, P., Kraus, D., & Chen, B. (2015). Aminolevulinic acid-based tumor detection and therapy: molecular mechanisms and strategies for enhancement. *International Journal of Molecular Sciences*, 16(10), 25865-25880. DOI: [10.3390/ijms161025865](https://doi.org/10.3390/ijms161025865)

Yip-Schneider, M. T., & Schmidt, C. M. (2003). MEK inhibition of pancreatic carcinoma cells by U0126 and its effect in combination with sulindac. *Pancreas*, 27(4), 337-344. DOI: [10.1097/00006676-200311000-00012](https://doi.org/10.1097/00006676-200311000-00012)

Yoshioka, E., Chelakkot, V. S., Licursi, M., Rutihinda, S. G., Som, J., Derwish, L., King, J. J., Pongnopparat, T., Mearow, K., Larijani, M., Dorward, A. M., & Hirasawa, K. (2018).

Enhancement of Cancer-Specific Protoporphyrin IX Fluorescence by Targeting Oncogenic Ras/MEK Pathway. *Theranostics*, 8(8), 2134–2146. DOI: [10.7150/thno.22641](https://doi.org/10.7150/thno.22641)

Zhao, H., Cui, K., Nie, F., Wang, L., Brandl, M.B., Jin, G., Li, F., Mao, Y., Xue, Z., Rodriguez, A., & Wong, S. T. (2012). The effect of mTOR inhibition alone or combined with MEK inhibitors on brain metastasis: an in vivo analysis in triple-negative breast cancer models. *Breast Cancer Research and Treatment*, 131(2), 425-436. DOI: [10.1007/s10549-011-1420-7](https://doi.org/10.1007/s10549-011-1420-7)

Zhao, S., Wu, J., Wang, C., Liu, H., Dong, X., Shi, C., Shi, C., Liu, Y., Teng, L., Han, D., & Chen, X. (2013). Intraoperative fluorescence-guided resection of high-grade malignant gliomas using 5-aminolevulinic acid-induced porphyrins: A systematic review and meta-analysis of prospective studies. *PloS One*, 8(5), e63682. DOI: [10.1371/journal.pone.0063682](https://doi.org/10.1371/journal.pone.0063682)

Zhao, Y., & Adjei, A. A. (2014). The clinical development of MEK inhibitors. *Nature Reviews Clinical Oncology*, 11(7), 385. DOI: [10.1038/nrclinonc.2014.83](https://doi.org/10.1038/nrclinonc.2014.83)

Zheng, Y., Yang, H., Wang, H., Kang, K., Zhang, W., Ma, G., & Du, S. (2019). Fluorescence-guided surgery in cancer treatment: current status and future perspectives. *Annals of Translational Medicine*, 7(Suppl 1). DOI: [10.21037/atm.2019.01.26](https://doi.org/10.21037/atm.2019.01.26)

Zhou, S., Zong, Y., Ney, P. A., Nair, G., Stewart, C. F., & Sorrentino, B. P. (2005). Increased expression of the Abcg2 transporter during erythroid maturation plays a role in decreasing cellular protoporphyrin IX levels. *Blood*, 105(6), 2571-2576. DOI: [10.1182/blood-2004-04-1566](https://doi.org/10.1182/blood-2004-04-1566)

Zhou, Y., Hu, H.Y., Meng, W., Jiang, L., Zhang, X., Sha, J.J., Lu, Z., & Yao, Y. (2014). MEK inhibitor effective against proliferation in breast cancer cell. *Tumor Biology*, 35(9), 9269-9279. DOI: [10.1007/s13277-014-1901-5](https://doi.org/10.1007/s13277-014-1901-5)

Appendix



Animal Care Committee (ACC)

St. John's, NL, Canada A1C 5S7

Tel: 709 777-6620 acs@mun.ca

<https://www.mun.ca/research/about/acs/acc/>

Dear: Dr. Kensuke Hirasawa, Faculty of Medicine\Division of BioMedical Sciences

Researcher Portal File No.: 20210094

Animal Care File: 20-11-KH

Entitled: (20-11-KH) Efficacy of MEK inhibition on in vivo photodynamic therapy

Status: Active

Related Awards:

Awards File No	Title	Status	
20140499	Cancer cell fluorescence screening for ancolytic virus sensitivity	Completed	1. Research Grant and Contract Services (RGCS) – St. John's and Grenfell Campuses
20141501	Exploiting modulation of PpIX accumulation by Ras/MEK: an innovative approach towards photodynamic therapy	Active	1. Research Grant and Contract Services (RGCS) – St. John's and Grenfell Campuses
20160832	Targeting cancer stem cells with photodynamic therapy	Active	1. Research Grant and Contract Services (RGCS) – St. John's and Grenfell Campuses
20161641	Targeting cancer stem cells with photodynamic therapy	Completed	1. Research Grant and Contract Services (RGCS) – St. John's and Grenfell Campuses
20161902	Targeting cancer stem cells with photodynamic therapy	Active	1. Research Grant and Contract Services (RGCS) – St. John's and Grenfell Campuses
20181342	Enhancing 5-ALA-PDT efficacy by MEK	Completed	1. Research Grant and Contract Services (RGCS) – St. John's and Grenfell Campuses

20181382	Evaluation of combined photodynamic therapy with a MEK inhibitor in animal cancer models	Completed	1. Research Grant and Contract Services (RGCS) – St. John's and Grenfell Campuses
20182170	Improving photodynamic diagnosis and therapy by targeting the MEK-ABCB1 axis	Active	1. Research Grant and Contract Services (RGCS) – St. John's and Grenfell Campuses
20200595	Restoring 5-ALA-PDT Sensitivity through MEK Inhibition in in-vitro and in-vivo systems.	Completed	1. Research Grant and Contract Services (RGCS) – St. John's and Grenfell Campuses
20200897	Targeting oncogenic Ras/MEK to promote photodiagnosis and photodynamic therapy efficacy	Pending Sponsor Decision	1. Research Grant and Contract Services (RGCS) – St. John's and Grenfell Campuses

Ethics Clearance Terminates: January 10, 2023

Your Animal Use Protocol has been renewed for a three-year term. This file replaces File ID [[20171352]] and Animal Care ID [[17-11-KH]] as the active ethics clearance associated with this project. Note the new file ID and Animal Care ID when referring to this protocol.

Also, please be informed that the 2 cell lines (4T1 and DLD-1) must be tested before use. Cell lines are tested once, and there is confirmation from your research team that these 2 cell lines have not been tested.

This ethics clearance includes the following Team Members: Dr. Kensuke Hirasawa (Principal Investigator)

Vipin Shankar Chelakkot Govindalayathil (Co-Investigator)

This ethics clearance includes the following related awards:

Awards File No	Title	Status	
20140499	Cancer cell fluorescence screening for ancolytic virus sensitivity	Completed	1. Research Grant and Contract Services (RGCS) – St. John's and Grenfell Campuses
20141501	Exploiting modulation of PpIX accumulation by Ras/MEK: an innovative approach towards photodynamic therapy	Active	1. Research Grant and Contract Services (RGCS) – St. John's and Grenfell Campuses
20160832	Targeting cancer stem cells with photodynamic therapy	Active	1. Research Grant and Contract Services (RGCS) – St. John's and Grenfell Campuses
20161641	Targeting cancer stem cells with photodynamic therapy	Completed	1. Research Grant and Contract Services (RGCS) –

			St. John's and Grenfell Campuses
20161902	Targeting cancer stem cells with photodynamic therapy	Active	1. Research Grant and Contract Services (RGCS) – St. John's and Grenfell Campuses
20181342	Enhancing 5-ALA-PDT efficacy by MEK	Completed	1. Research Grant and Contract Services (RGCS) – St. John's and Grenfell Campuses
20181382	Evaluation of combined photodynamic therapy with a MEK inhibitor in animal cancer models	Completed	1. Research Grant and Contract Services (RGCS) – St. John's and Grenfell Campuses
20182170	Improving photodynamic diagnosis and therapy by targeting the MEK-ABCB1 axis	Active	1. Research Grant and Contract Services (RGCS) – St. John's and Grenfell Campuses
20200595	Restoring 5-ALA-PDT Sensitivity through MEK Inhibition in in-vitro and in-vivo systems.	Completed	1. Research Grant and Contract Services (RGCS) – St. John's and Grenfell Campuses
20200897	Targeting oncogenic Ras/MEK to promote photodiagnosis and photodynamic therapy efficacy	Pending Sponsor Decision	1. Research Grant and Contract Services (RGCS) – St. John's and Grenfell Campuses

An Event [Annual Report] will be required following each year of protocol activity.

Should you encounter an unexpected incident that negatively affects animal welfare or the research project relating to animal use, please submit an Event [Incident Report].

Any alterations to the protocol requires prior submission and approval of an Event [Amendment].

NOTE: You can access a copy of this email at any time under the “Shared Communications” section of the Logs tab of your file in the [Memorial Researcher Portal](#).